UNIVERSITY OF LEEDS

Article:
Lentzakis, H, Costanzo, S, Vlassopoulos, D et al. (5 more authors) (2019) Constraint Release mechanisms for H-Polymers moving in Linear Matrices of varying molar masses. Macromolecules, 52 (8). pp. 3010-3028. ISSN 0024-9297

https://doi.org/10.1021/acs.macromol.9b00251

Constraint Release mechanisms for H-Polymers moving in Linear Matrices of varying molar masses

Helen Lentzakis[1,*], Salvatore Costanzo[1,**], Dimitris Vlassopoulos[1], Ralph H. Colby[2], Daniel Jon Read[3], Hyojoon Lee[4], Taihyun Chang[4], Evelyne van Ruymbeke[5,***]

[1]: Institute of Electronic Structure & Laser, Heraklion, Foundation for Research and Technology Hellas (FORTH), Crete 70013, Greece, and Department of Materials Science & Technology, University of Crete, Heraklion, Crete 70013, Greece

[2]: Department of Materials Science and Engineering, The Pennsylvania State University, University Park, PA 16802 USA

[3]: Department of Applied Mathematics, University of Leeds, Leeds, LS2 9JT UK

[4]: Pohang University of Science and Technology, Department of Chemistry and Division of Advanced Materials Science, Pohang, 37673, Korea

[5]: Bio and Soft Matter, Institute on Condensed Matter and Nanosciences (IMCN), Université catholique de Louvain (UCL), Louvain 1348, Belgium

* Present address: Kruger Inc., Montreal QC H3S 1G5, Canada

** Present address: University of Naples Federico II, DICMAPI, P. le Tecchio 80, Naples 80125, Italy

***: Evelyne.vanruymbeke@uclouvain.be

Abstract

We investigate the influence of the environment on the relaxation dynamics of well-defined H-polymers diluted in a matrix of linear chains. The molar mass of the linear chain matrix is systematically varied and the relaxation dynamics of the H-polymer is probed by means of linear viscoelastic measurements, with the aim to understand its altered motion in the different blends, compared to its pure melt state. Our results indicate that short unentangled linear chains accelerate the relaxation of both the branches and the backbone of the H-polymers by acting as an effective solvent. On the other hand, the relaxation of the H-polymer in an entangled matrix is slowed-down, with the degree of retardation depending on the entanglements number of the linear chains. We show that this retardation can be quantified by considering that the H-polymers are moving in a dilated tube at the rhythm of the motion of the linear matrix.

I. Introduction

The tube model of Doi, Edwards and de Gennes[1-3] provides the framework for a molecular understanding of the relationship between the topological structure of entangled polymer systems and their flow properties. The linear rheology of monodisperse entangled linear polymers is well understood and can be predicted with state-of-the-art tube-based molecular models[4-7]. However, the current tube models are not yet at the level of refinement where they can universally predict the linear rheology of blends of two or more monodisperse polymers. Most of the literature has focused on binary linear blends[8-23] and blends of linear and star polymers[24-32]. The underlying physics governing the blend relaxation is the constraint release (CR) effect of the faster relaxing short chains on the slower long chains[10]. When changing the molecular structure of the probe (slower) polymer, CR may have a different influence on non-reptative terminal relaxation. However, other than experimental studies involving star and linear mixtures, there are only a few other studies of binary mixtures of well-characterized architecturally complex polymers[33-35]. Yet, such blends are encountered in all

technological applications. In this work, we wish to further understand the relaxation of such complex polymer blends by studying the viscoelastic response of a model H-polymer blended into linear chain matrices of different molar masses. The choice of the particular probe molecule is based on the fact that it is the simplest branched polymer after the stars, having two well-defined branching points. The established pom-pom polymer[36,37] is nothing more that the H-polymer with more than two branches grafted in the ends of the linear backbone.

The underlying problem with these models is the uncertainty around the interpretation of CR in describing the effect of the relaxation of surrounding chains on the motion of the tube surrounding the probe chain. Examples of models which interpret CR include "self-consistent constraint release" [4,8], "double reptation"[38,39], "constraint release Rouse"[11,40] and "dynamic tube dilation"[41,42]. Although they have shown to be successful in limited cases, these models are not universal for all types of blends, i.e., for a wide range of volume fractions and relaxation times of the respective monodisperse components. For instance, most tube model theories for polydisperse systems include a full dynamic tube dilation theory (DTD)[37,41-43] where the relaxed segments are immediately taken as a solvent and act to enlarge the tube. However, as was recently demonstrated[17-19,33,44,45], it may be that only partial DTD is needed in order to provide a universal molecular picture for polydisperse polymers. Watanabe demonstrated that full DTD is only applicable in the blend case of two monodisperse linear polymers where the components have widely separated relaxation times. Thus, from this example, it seems evident that the short component in polymer blends cannot always be considered as solvent for the relaxation of the long component, and that clear criteria are needed which allow determining the effective fraction of relaxed polymer diluting the entanglement network experienced by the slower polymers.

A first criterion has been proposed by Struglinsky and Graessley[10] in the specific case of binary linear blends. According to this criterion, relaxation of the long component takes place at a rate dictated by constraint release events only if the motion and renewal of the tube due to the loss/renewal

of topological constraints, known as (thermal) Constraint Release[11,40], is much faster than the reptation of the long chains in their initial (thin) tube. In order to compare these times, the authors propose a new parameter, called the "Struglinsky-Graessley' parameter, r_{SG}, defined as the ratio of the reptation time of the long chains in an undilated tube ($\tau_L=3\tau_e Z_L^3$, with τ_e the relaxation time of a segment between two entanglements and Z_L, the number of entanglements per long chain) and the Constraint Release Rouse time of this long component if it is diluted in a matrix of short chains ($\tau_{CRR}=\tau_S Z_L^2$, with $\tau_S=3\tau_e Z_S^3$, the reptation time of the short chain):

$$r_{SG} = \frac{Z_L}{{Z_S}^3} = \frac{M_L {M_e}^2}{{M_S}^3} \quad (1)$$

where M_L and M_S are the molecular weights of the long and short linear polymer chains, respectively. It must be noted that this criterion does not take into account the possible influence of the Contour Length Fluctuations (CLF) mechanism, which is known to significantly reduce the relaxation time of the long chains if these last ones contain few long-long entanglements (< 20). For dilute long chains, when the r_{SG} value is smaller than a critical value, then reptation of the long chains occurs along the thin tube, otherwise, the long chains relax by Constraint Release Rouse faster than they can relax by reptation. Hence, according to this criterion, the CR mechanism can be properly analyzed only if there is a distinct separation of time scales. However, in reality, this is often not the case. Furthermore, the critical value of r_{SG} at which the transition takes place, from reptation in a thin tube to CR Rouse motion, is not accurately defined, and seems to be much lower than 1. For example, a critical value of 0.1 was determined from diffusivity measurements[46], while Park and Larson[21] found a value of 0.064 to be applicable in linear viscoelastic data. Also, this value does not account for the influence of contour length fluctuations of the short component. Tracer diffusion data for the long chains diffusing in a matrix of short chains demonstrated that reptation is

the dominant diffusion mechanism when short chains molar mass is above a critical value, whereas at smaller values, the diffusion coefficient associated with CR dominates[46]. Upon further review, Green and Kramer[47] accounted additionally for contour length fluctuations and could also predict the crossover in Green's diffusion data[48].

For more concentrated long chains, full relaxation by CR Rouse motion is prevented by entanglements between the long chains. Once the long component has occupied its dilated tube (which is only formed by the entanglements between long chains), further relaxation is either via reptation along the thin tube, or reptation (of the chain or of the thin tube) along a dilated tube formed by the entanglements between long chains, at a rate dictated by CR events. Reptation along the dilated tube is expected to occur at values of r_{SG} greater than the number of entanglements along the dilated tube[16,49].

Others such as Liu et al.[23] have experimentally explored the consequences of CR on chain dynamics. To this end, they have essentially switched-off CR events by properly choosing blends with specific ratios of characteristic times of the components, say a short one and a much longer representing an effective 'sea' of fixed constraints. This type of study allows quantifying the "amount" of CR and is known as probe dynamics. Indeed, when dilute short entangled polymer chains are added to a melt of long chains, the constraint release associated with the short chain entanglements can be effectively switched-off. Therefore, this situation is analogous to a mixture of dilute polymer chains in a cross-linked network[23,50]. Probe rheology on binary blends as a tool to determine the CR effects was also studied by Watanabe et al.[19] and Matsumiya et al.[44] by confronting viscoelastic and dielectric data of such blends, as well as by other authors[51]. In all these works, it was found that there is a retardation (slowing down) of the terminal relaxation time of the short polymer chains in the environment of long polymer chains. This demonstrates the important role of CR in speeding-up the relaxation processes (reptation or arm retraction).

From the above, it is evident that one needs to distinguish the CR events in a blend. Taking the example of earlier works[2,17,18,49], Read et al.[15,16] have simplified the CR picture by assigning only two constraint release states, corresponding to two specific tube diameters, as first proposed long ago[2,49]: the first state represents the long chains entangled with all other chains, while the second state only takes into account the entanglements of the long chains with other long chains. Thus, the simplified tube-based picture (Figure 1) is that of two tubes, one 'thin' tube (representative of all entanglements) contained in a 'fat' (dilated) tube (representative of entanglements involving only the long chains). According to the SG criterion, the long chains reptate in the dilated tube ($\upsilon_L^{-\alpha/2}$ larger than the thin tube, with υ_L being the weight fraction of long chains and α, the dynamic dilution exponent) only if the Struglinsky-Graessley parameter r_{SG} is larger than the number of entanglements in the fat tube, otherwise their reptation will occur in the thin tube with no tube dilation .

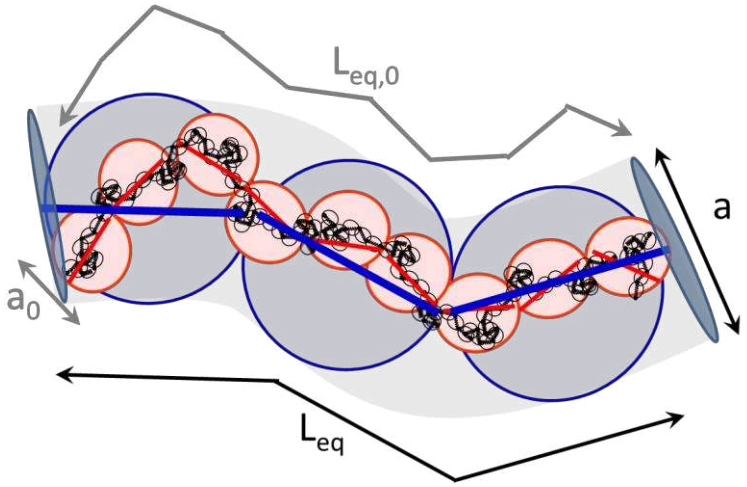

Figure 1: Probe chain in a thin tube (taking into account all entanglements of long chains) trapped in a dilated tube (only based on the entanglements between the long chains). There are two possibilities of long chain reptation: either in the thin tube with tube diameter a_0 and length $L_{eq,0}$ or in the dilated tube with tube diameter $a = a_0\upsilon_L^{-\alpha/2}$ and length $L_{eq} = L_{eq,0}\upsilon_L^{\alpha/2}$.

This simplified description of CR, has been successfully used to model both linear viscoelasticity and nonlinear and elongational rheology of several bidisperse linear blends[15,16,52]. A similar picture of thin and dilated tube was also used by van Ruymbeke et al.[13,14] and Ebrahimi et al.[31] for modelling the viscoelastic behavior of binary linear blends with well separated molar masses. In these models, it is assumed that the long chains can either move and relax in their thin tube, or relax in their fat tube but only at the rhythm of the destruction/re-construction of the entanglements involving short chains. Thus, while the contour length of the fat tube is shorter than that of the initial tube (see Figure 1: $L_{eq}/L_{eq,0} = \upsilon_L^{\alpha/2}$), which speeds up reptation and CLF processes, the Rouse time associated with a long-long entanglement segment (i.e., a segment between two entanglements of long chains), $\tau_{long-long,e}$, is longer than its intrinsic Rouse time (equal to τ_e/υ_L^2) since it depends on the lifetime of a long-short entanglement, $\tau_{long\text{-}short}$ and on the number of such entanglements per long-long entanglement segment, υ_S/υ_L.[31]

$$\tau_{long-long,e} = max\left(\frac{\tau_e}{\upsilon_L{}^2},\ \tau_{long-short}\left(\frac{\upsilon_S}{\upsilon_L}\right)^2\right), \quad (2)$$

with υ_S being the weight fraction of short chains. These slow motions in a fat tube lead to extra relaxation processes, defined as the CR-activated CLF and CR-activated reptation processes, which take place in addition to the relaxation of the chains in their thin tube[14-16,53].

As shown in ref. [13,14, 53], when the CR-activated CLF has a large influence on the relaxation of long chains, an enhanced effect of CR process from the short chains is measured, corresponding to an experimentally determined apparent dynamic dilution exponent α_{exp}, which takes values close to 4/3 (as determined based on the evolution of the terminal modulus). Whereas this issue remains unsettled, it has been shown recently that by accounting for CR-CLF process, the viscoelastic

properties of all these binary linear blends with well-separated molar masses can be correctly predicted with a (theoretically determined) dynamic dilution exponent $\alpha = 1$.[14, 53,54]

The objective of the present work is to extend the investigation of CR effect in more complex polymer blends, involving branched polymers which display hierarchical relaxation of their different generations of branches in the monodisperse state and a respective tunable nonlinear response (for example, extension hardening). To this end, we investigate the relaxation dynamics of binary mixtures of entangled H-polymer (the probe)[55] in linear polymers (the matrix) of varying molar mass. In order to ensure working with model systems, a combination of state-of-the art synthesis, characterization tools and careful rheological measurements is needed. The specific H-polymer used in this study (coded as H3A1) is nearly monodisperse and its linear viscoelastic properties have been well reported in the past[7,55,56]. In the melt state, the H-polymer undergoes hierarchical relaxation where the four arms retract by fluctuations and act as a solvent for the backbone which eventually relaxes only after the arms have fully retracted[36]. Additional friction coming from the branches must be taken into account in the backbone relaxation, both in reptation (center of mass diffusion of chains out of their tube) and in CLF processes[7]. In addition, there are continuously constraint release events occurring when relaxed segments release topological constraints on unrelaxed segments thus speeding up their relaxation process[57, 58, 59]. While the H3A1 polymer is in a very long linear matrix, constraint release events on the H-polymer should be turned off and consequently its relaxation should be slowed down. In contrast, the H-polymer in a short linear matrix should demonstrate a speeding up of the relaxation of the H-polymer due to additional constraint release events from the surrounding short chains. Quantifying these effects is a real challenge that we would like to address in this work.

In order to systematically investigate the influence of CR, we have selected several sets of H/linear blends: first, by using unentangled linear chains, the H-polymers are

expected to relax as in a real solvent. Therefore, at low concentration of H-polymers, we can investigate the Rouse dynamics of such H-polymers. Then, by gradually increasing the molar mass of the linear chains and by varying the concentration of H-polymers, we aim at understanding and quantifying the expected retardation θ_{matrix} of the relaxation of the H-polymers, compared to their relaxation in an unentangled matrix, and discuss the range of validity of our results. The paper is organized as follows: Section II is an experimental section which includes details of the preparation of the mixtures and the methods of characterization such as DSC and Small Oscillatory Shear measurement (SAOS). In Section III, the experimental linear viscoelastic data of the different samples are presented and discussed. Based on the experimental results, we develop a model in Section IV in order to describe the relaxation of such blends. In Section V, the data are analyzed and discussed, based on this model. Conclusions and Perspective are presented in Section VI.

II. Experimental

II.1 Materials. The H-polymer and linear polymers were all synthesized by anionic polymerization under high vacuum. In the first blend series, the H-polystyrene H3A1, which was studied in ref. [55], was blended with a series of linear polystyrenes (PS) with varying molar mass (obtained either from Polymer Source (Montreal, Canada) or Polymer Standard Service (Mainz, Germany)). The molecular characteristics of the H-polymer are listed in Table 1, while those of the linear polymers are listed in Table 2.

The purity of the sample was checked by temperature gradient interaction chromatography (TGIC) since this technique allows efficiently separating polymers of different molar masses with much higher resolution than size exclusion chromatography. As detailed in refs. [60-62], it is based on temperature dependent adsorptive interaction of polymers to the stationary phase. TGIC chromatogram of H3A1 is shown in Figure 2. Well-overlapped chromatograms recorded by UV

(A_{260}) and light scattering (R_{90}) detectors indicate that the polymer has a very narrow dispersity. The dispersity determined by the light scattering detection is lower than 1.01.

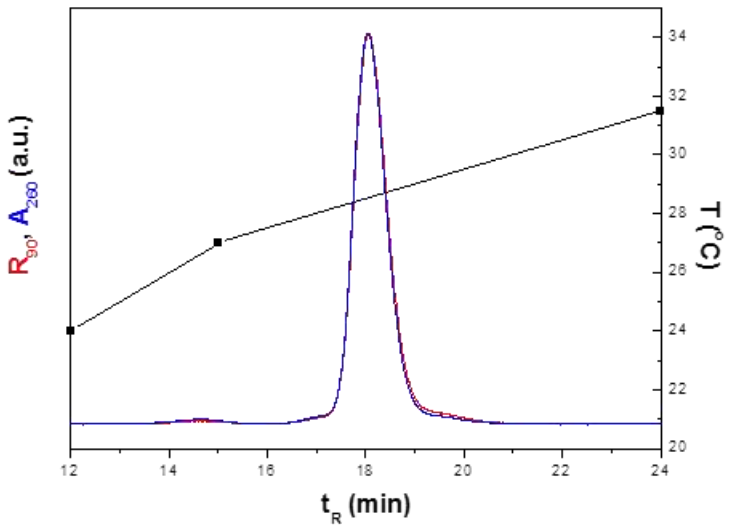

Figure 2: TGIC chromatogram of the H polystyrene H3A1. Separation condition: Nucleosil C18 (150 x 4.6 mm, 500 Å, 7 μm), CH_2Cl_2/CH_3CN (58/42. v/v) at 0.5 mL/min. Temperature program is shown in the plot.

The linear PS samples with narrow dispersity were blended with H3A1, the latter being at volume fractions υ_H = 1.5%, 3% and/or 10% (Table 2). The volume fraction was calculated as the ratio of the mass of H3A1 m_H and the total mass m_T of the blend, since the densities of linear and H-PS are the same. The conformation of flexible polymers can be described as random walks and the ratio of their mean square end-to-end distance $\langle R^2 \rangle_0$ and their molar mass is a constant. For PS, $\langle R^2 \rangle_0/M$ = 0.0043 nm^2.[63] In order to calculate the radius of gyration of H-PS, we use Kramer's theorem and follow the procedure of Colby and Rubinstein[8], according to which the radius of gyration R_g of an H-polymer is:

$$R_g = b\sqrt{\frac{\left(\frac{N_a}{2}+N_b\right)^2}{2(N_a+N_b)} - \frac{1}{3(N_a+N_b)^2}\left[\left(\frac{N_a}{2}+N_b\right)^3 - \frac{{N_a}^3}{48}\right]} \quad (3)$$

where b is the Kuhn length and $N_a/4$ and N_b are the number of Kuhn monomers of each arm and the backbone, respectively. The resulting value is R_g=18 nm. With the monomer volume V_0 of PS being 1.2 nm^3, the overlap volume fraction, defined as the ratio of the chemical (occupied) volume of a single polymer to the pervaded volume of the polymer chain, is:

$$\phi^* = \frac{V_0(N_a+N_b)}{\frac{4}{3}\pi {R_g}^3} \quad (4)$$

For the present H-PS in theta solvent conditions, $\phi^* \approx 4.4\%$.

The samples were carefully weighed, sufficient toluene or tetrahydrofuran (THF) was added in order to completely dilute the mixture and the blend was slowly mixed (for a minimum of one day). In general, mixing was performed using a tumbler and THF was gradually replaced by toluene. To avoid the risk of degradation, the amount of THF was kept to a minimum. Following mixing, the solvent was evaporated, first slowly and then more rapidly as the temperature was gradually increased well above the glass transition temperature in a well-sealed vacuum oven. This procedure ensured complete evaporation of the entire solvent, as checked by monitoring the mass of the mixture.

The molar mass between entanglements M_e in Table 1 has been set to 14.8 kg/mol, based on the analysis of monodisperse samples with the time marching algorithm (TMA) tube model, as well as previous works with entangled PS samples[58]. In the framework of tube model analysis, the value of the plateau modulus G_N^0 is then calculated from M_e, the mass density of the polymer ρ, the universal gas constant R and the temperature T:[65]

$$G_N^0 = \frac{4}{5}\frac{\rho RT}{M_e} \quad (5)$$

Its value was fixed to 0.23 MPa, consistently with [14, 64], which is close to the usual value proposed in literature, of 0.20 MPa.[63,66] In addition, the weight-average molar mass of an arm M_a, the number of branch points q, the number of entanglements per arm $Z_a = M_a/M_e$, the number of backbone entanglements $Z_b = M_b/M_e$, R_g and φ^* are listed in Table 1.

Table 1: Molecular Characteristics of H-polystyrene (from Roovers[55]) [1]

code	M_e	M_b (kg/mol)	Z_b	M_a (kg/mol)	Z_a	q	M_{total} (kg/mol)	R_g (nm)	ϕ^*
H3A1	14.8	123	8.3	132	8.9	2	674	18.6	0.04

[1] The molar masses are weight-averaged and the polydispersity is below 1.1.

Table 2: Molecular characteristics of H/linear polystyrene mixtures

Code of linear matrix	$M_{lin} = M_w$ of linear matrix [kg/mol]	M_w/M_n [4]	Volume fraction of H in the blends (υ_H)	$M_{w,total}$ [kg/mol] of the blends [5]
PS 5k [1]	5.1	1.08	1.5%, 3%, 10%	14.8, 24.5, 70
PS 22k [1]	22.2	1.07	1.5%, 3%, 10%	31.6, 41, 85
PS 64k [1]	64	1.06	1.5%, 3%, 10%	60, 70, 111
PS 129k [1]	129	1.04	3%, 10%	147, 181
PS 185k [2]	182	1.03	1.5%, 3%, 10%	189, 199, 229
PS 483k [2]	483	1.05	10%	500
PS 1 M [3]	1000	<1.1	10%	965

[1] from Polymer Source, Canada

[2] from Polymer Standard Service, Germany

[3] from University of Athens, Greece

[4] obtained via Size Exclusion Chromatography (see section II.3).

[5] average values estimated from the components

II.2 Differential Scanning Calorimetry (DSC). DSC measurements were performed in order to determine the glass temperature T_g of the different samples investigated. A standard calorimeter (PL-DSC from TA) was used and all the samples were heated and cooled at a rate of 10 °C/min. The first run was not considered, as is customary.

II.3 Size Exclusion Chromatography (SEC). For SEC analysis of the PS samples, two columns (Agilent, Mixed-B two-column set, 300 × 7.5 mm i.d.) were used at a column temperature of 40 °C. Eluent was THF (Samchun, HPLC grade) at a flow rate of 0.8 mL/min. SEC chromatograms were recorded with a light scattering (LS)/refractive index (RI)/viscometer (DP) (Viscotek TDA 302) and a UV absorption detector (TSP, UV2000 at 260 nm wavelength) for on-line determination of absolute molar mass of polymers. The dn/dc value for PS in THF is 0.185 mL/g. Polymer samples were dissolved in THF at a concentration of ~1 mg/mL, and the injection volume was 100 μL.

II.5 Small Amplitude Oscillatory Shear Results (SAOS). SAOS measurements were performed for the monodisperse and blend PS samples on an ARES 2KFRTN1 strain-controlled rheometer (TA Instruments, USA) at temperatures ranging from 110°C to 190°C with an Invar (a copper−iron alloy with low thermal expansion) parallel plate geometry of 8, 13 and 25 mm diameter. Temperature control was achieved with a convection oven yielding an accuracy of ± 0.1°C and the measurements were always performed in a nitrogen environment in order to reduce the risk of degradation. Time-temperature superposition (TTS)[67,68] was performed at a reference temperature of 130°C and the generated master curves allowed obtaining the relevant viscoelastic parameters, i.e., τ_e, G_N^0 and terminal relaxation time. Figure 3 depicts the temperature-dependent horizontal and vertical shift factors along with the fit of the former by means of the WLF equation[67]:

$$\log(a_T) = \frac{-C_1(T-T_{ref})}{C_2+T-T_{ref}} \quad (6)$$

The fit yielded C_1=8.4 and C_2=80°C at a reference temperature T_{ref} of 130°C, consistent with literature values when compared to the same reference temperature[35,67,69]. The vertical (modulus-scale) shift factors b_T were calculated from the density compensation[67]:

$$b_T = \frac{\rho(T)(T)}{\rho(T_{ref})(T_{ref})} \quad (7)$$

with the temperature-dependent density being[70]:

$$\rho(T) = 1.2503 - 6.05\ 10^{-4}(T) \quad (8)$$

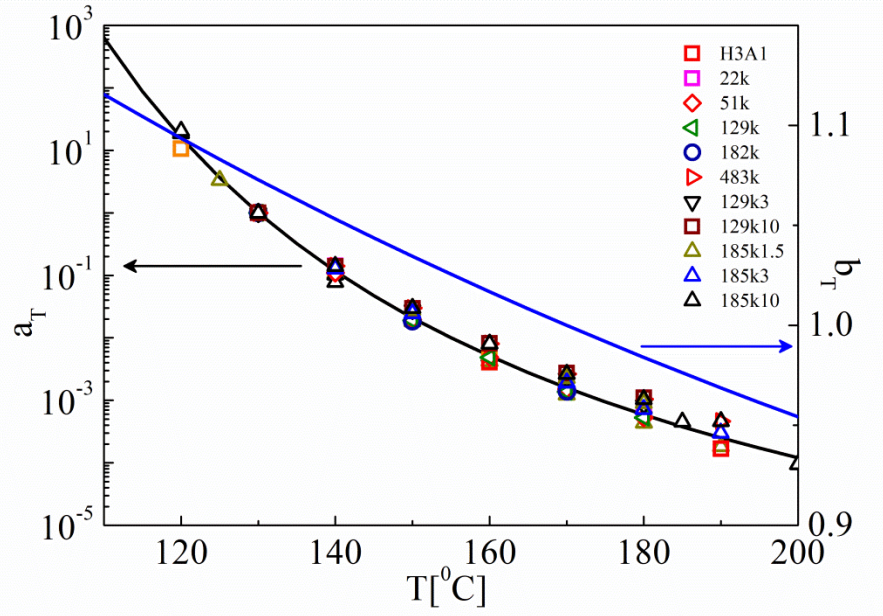

Figure 3: Horizontal a_T and vertical b_T shift factors associated to the PS linear and blend samples at T_{ref}=130°C.

Creep measurements were performed in order to extend the range of probed time scales where dynamic measurements were limited by the minimum torque resolution of the rheometer or by thermal degradation of the samples. Creep experiments were performed on a Physica MCR702 rheometer (Anton Paar GmbH, Germany), equipped with a hybrid temperature control unit

(CTD180) which combines a Peltier element with gas convection. Nitrogen atmosphere was used to prevent degradation upon heating. For each sample, two different creep experiments were performed, with two different levels of the applied stress. The overlap of the resulting creep compliances demonstrated that the tests were carried out in linear conditions. The creep compliance was converted into dynamic moduli by means of the NLreg software, based on the Tikhonov regularization method[65].

III Experimental Results

III.1 DSC. Table 3 depicts the measured glass temperatures of nearly all samples. As expected, a difference in T_g between the lowest-M_w and the highest-M_w linear PS sample is observed. It is typically described by the Fox-Flory equation $T_g=T_{g,\infty}-C/M_n$, where $T_{g,\infty}$ is the limiting glass temperature at high molar mass, $C=1.1x10^5$ gK/mol is constant depending on chemistry and M the molar mass.[72,73]. Here we take $T_{g,\infty}$=107°C based on the data of Table 3 (about 10% higher than that reported by Rubinstein and Colby[72], apparently due to the calibration of the DSC instrument used). The data of Table 3 do follow the predicted dependence on molar mass of T_g. Since T_g differences correspond to horizontal shift in the SAOS frequency axis, comparison of linear and blend viscoelastic curves with respect to one another requires to horizontally shift the PS22k, the PS64k and the PS1000k curves in order to obtain the same temperature difference between the reference temperature T_{ref} of the master curves and their respective glass transition temperatures, (T_{ref} - T_g). The average T_g value of 106°C was chosen as the reference transition temperature $T_{g,ref}$. As expected, the barely entangled linear PS22k has a lower T_g (of 103±1°C) compared to $T_{g,ref}$. Since in this case, the (T_g-$T_{g,ref}$) difference corresponds to -3°C, the PS22k data have been shifted to T_{ref} - 3°C=127°C. The shift factor needed in order to compensate this difference is evaluated to be 0.47, while it is equal to 0.6 for PS64k which has a T_g of 104±1°C. In contrast, PS1000k has a higher T_g

value of 107±1°C and a corresponding shift factor of 1.3. Concerning the mixtures, their T_g values are rationalized by the Fox mixing rule $1/T_{g,blend}=w/T_{g,1}+(1-w)/T_{g,2}$, where 1 and 2 refer to the two constituents of the blend and w is the weight fraction[74].

Table 3: Glass temperatures as obtained by DSC

Linear and blend PS	T_g (°C)
PS 22k	103±1
PS 64k	104±1
PS 185k	106±1
PS 1000k	107±1
H3A1	105.5
PS 129k10% H3A1	106±1
PS 185k10% H3A1	106±1

III.2 Linear viscoelasticity

III.2.1 Monodisperse Polymers: In order to study the viscoelastic properties of the H-polystyrenes diluted in the different linear matrices, it is important to first determine the behaviour and main relaxation times of the monodisperse components. Their rheological data are shown in Figure 4. For the monodisperse H-polymer, one can observe two different relaxation peaks (or more accurately, two different shoulders) in the loss modulus curve (shown in the figure by arrows): the first peak corresponds to the arm retraction process and the second shoulder observed at lower frequency, is representative of the relaxation of the backbone. However, while these two peaks are detectable, they are not well-separated. Similarly, in the corresponding storage modulus G', one can hardly see the two plateau regimes that are expected from the hierarchical relaxation of such an architecturally complex macromolecule. This is due to the large number of arm entanglements, which makes the

backbone heavily diluted by the (relaxed) arms. Indeed, the volume fraction of the inner part of the backbone, υ_b, is only of 19% and its number of entanglements, Z_b, is approximately 8. Therefore if we consider full Dynamic Tube Dilation (DTD) and assume that the branches are fully relaxed, the effective number of entanglements of the (dynamically diluted) backbone $Z_{b,dil}= Z_b\upsilon_b^{\alpha}$, , reduces to only 1.6. This means that the backbone chains are nearly unentangled (with other backbone chains) and relax rapidly after the relaxation of the branches.

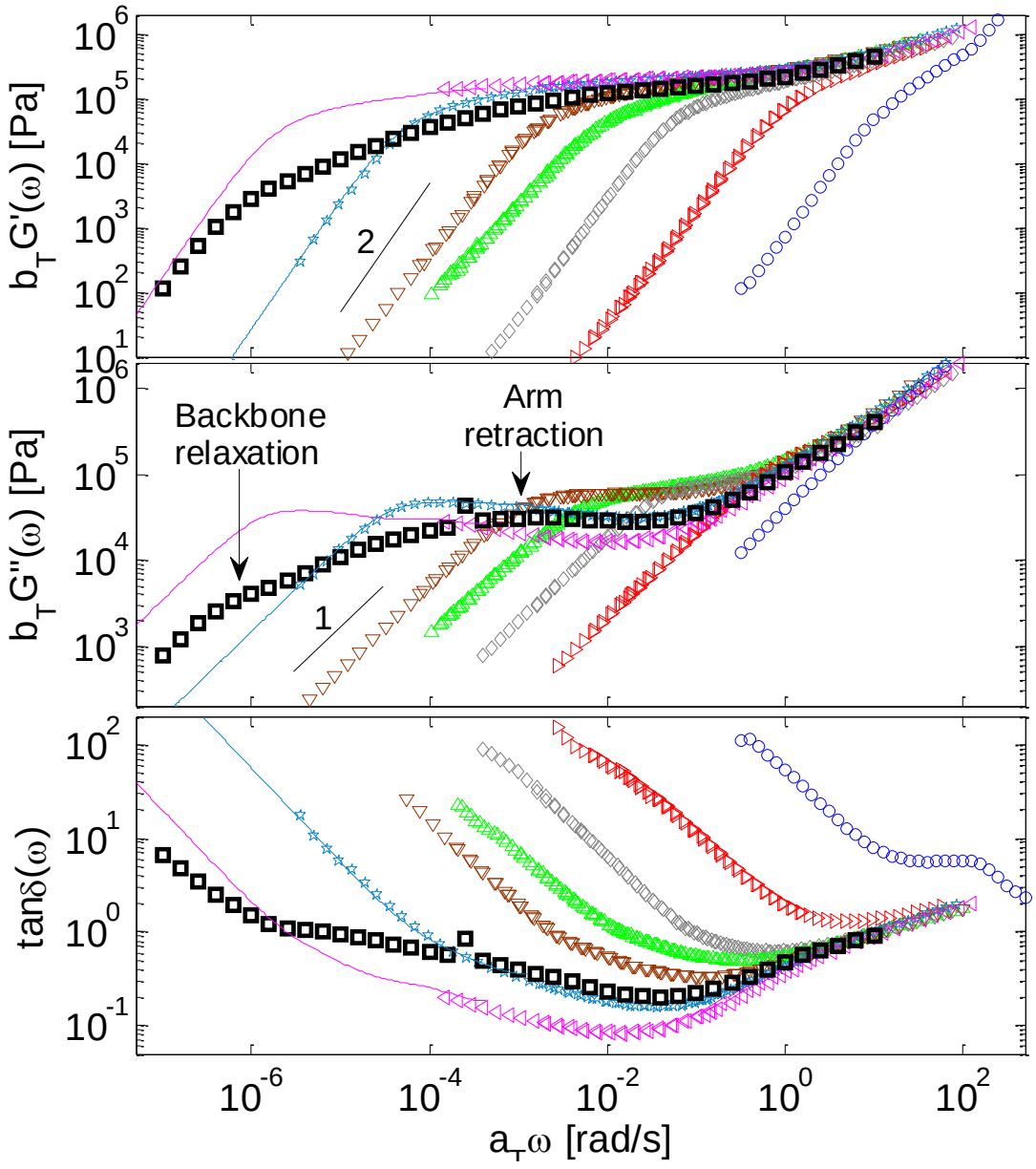

Figure 4: Experimental storage and loss moduli and tanδ master curves of H-PS sample H3A1 (thick black □) and of the linear matrices (5k (blue o), 22k(red >), 64k (grey ◊), 129k (green Δ), 185(brown ∇), 483k (cyan ∗) and 1000k (violet <)), at the reference temperature of 130°C for samples PS 64k, PS 129k, PS 185k and PS483k, respectively, and at iso-T_g condition for the other samples, with (T_{ref} - T_g) = 24°C (see section III.1). Continuous curves represent data obtained from creep measurements. The arrows indicate the relaxation peaks of the arms and backbone of the H polymer.

Figure 4 also compares the linear viscoelastic master curves of the seven linear monodisperse PS matrices (5k, 22k, 64k, 129k, 185k, 483k and 1000k) with that of H3A1. The timescale separation between the linear and probe arm and backbone relaxations is critically important for the assessment of constraint release. The main relaxation features of the linear polymers are directly observed in the rheological data. The G'(ω) and G''(ω) moduli for the PS linear 5k and 22k, whose M_w is below or roughly equal to M_e, does not show any rubbery plateau and exhibits a Rouse relaxation. The other well-entangled PS linear samples have a characteristic plateau modulus (which extends with increasing M_w) and a characteristic $G'=G''$ crossover relaxation time at $\tau_{lin}=1/\omega_c$ (since the linear samples are monodisperse). In addition, the characteristic terminal slopes of 2 ($G'\sim\omega^2$) and 1 ($G'\sim\omega$) are observed at low frequency. Note that the low-frequency data of 129k exhibit weaker slopes, apparently due to some large-molar mass tail (despite the low polydispersity reported in Table 2). This however does not influence the message of the work and will not be further analyzed.

III.2.2 H-linear polymer blends: Figure 5 depicts the linear viscoelastic storage moduli of the binary blends composed of 10 wt% of sample H3A1 and 90% of linear PS samples. It is observed that the relaxation of the H-polymers diluted in a linear matrix with $M_w \leq 185$ kg/mol is much faster

than in its pure H-environment (see Figure 4). Indeed, their characteristic rheological features are overshadowed by the relaxation of the linear polymer. This feature is due to the small amount of H-polymer in the blend, and can be explained as follows: as observed in Figure 5, the relaxation of the linear chains PS5k to PS185k takes place well before the time at which the retraction of the branches of H3A1 starts (at ω around 10^{-3} rad/s). Therefore, one could consider that for the corresponding blends, the linear matrix acts as a solvent for the terminal relaxation of the H-polymer. Under these conditions, the effective molar mass between two entanglements, M_e, after the relaxation of the linear matrix is equal to $M_{e,0}/\upsilon_H$ = 148 kg/mol, i.e., larger than the molar mass of the H-branches (132 kg/mol) and about 3 times smaller than the molar mass of the end-to-end longest path of the H-PS. Thus, for these blends, if DTD holds the H-polymers should relax according to a Constraint – Release Rouse (CRR) process, i.e., without the appearance of a second, low-frequency plateau. This hypothesis will be tested and discussed in Section V.

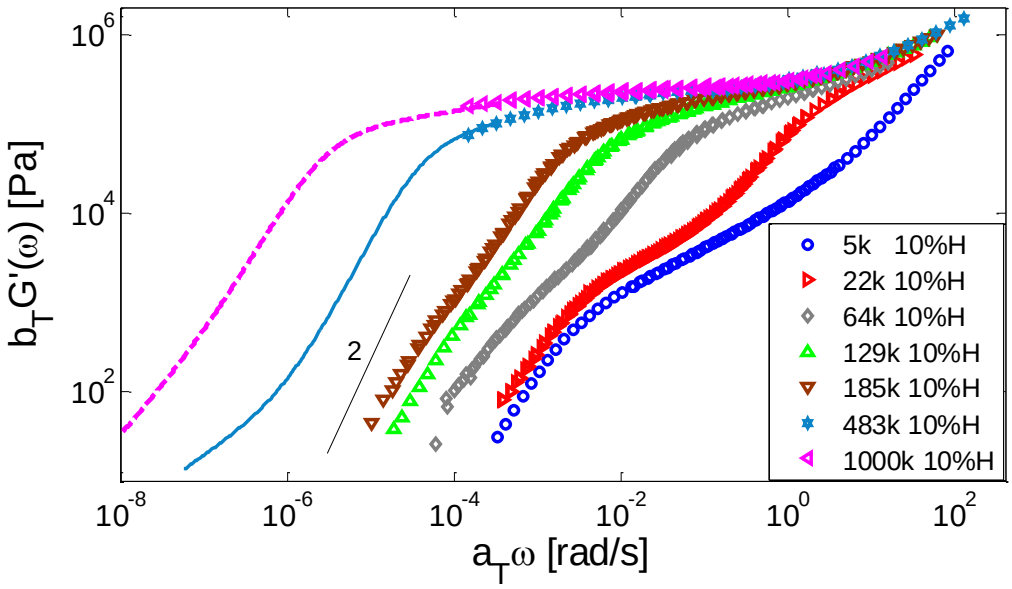

Figure 5: Linear viscoelastic storage modulus at T_{ref}=130°C of the binary blends composed of 10 wt% H3A1 and 90 st% of linear PS of varying M_w (5k, 22k, 64k, 129k, 185k, 483k and 1000k) samples. For samples 483k and 1000k, the continuous curves represent data obtained from creep

measurements. In the former case there is unambiguous evidence of the presence of a slow terminal mode (which is not fully detected), whereas in the latter case there is only a hint of possible (anticipated) slow mode.

On the other hand, Figure 5 shows that the blends of H-polymer in the shortest linear matrices exhibit the strongest effect in their G' (and G''). Indeed, the PS5k and the PS22k mixtures have noticeably different G'(ω) moduli compared to the linear monodisperse matrix (see Figure 4), with two distinct terminal relaxation modes. On the other hand, the presence of H-polymer in the longer matrices PS64k, PS129k and PS185k only leads to a weak, albeit unambiguous shoulder in the low-frequency data. This significant change observed in the shape of *G'* with the molar mass of the linear matrix already indicates that the relaxation of the H-polymers cannot be explained by considering their relaxation by CRR process together with the conventional definition of CRR time (i.e. $\tau_{CRR} = \tau_{lin} Z_H^2$, with τ_{lin} the relaxation time of the linear matrix and Z_H, the number of entanglements along the entire backbone of a H-polymer). Indeed, in such a case, the ratio ($\tau_{blend} / \tau_{lin}$) between the terminal time of the blend and the relaxation time of the linear matrix would have been constant for all the blends, which is obviously not the case. Instead, as illustrated in Figure 6, this ratio increases with decreasing molar mass of the linear chains, M_{lin}. A similar trend has been observed in other binary mixtures[9,31], and will be further discussed in Section V.

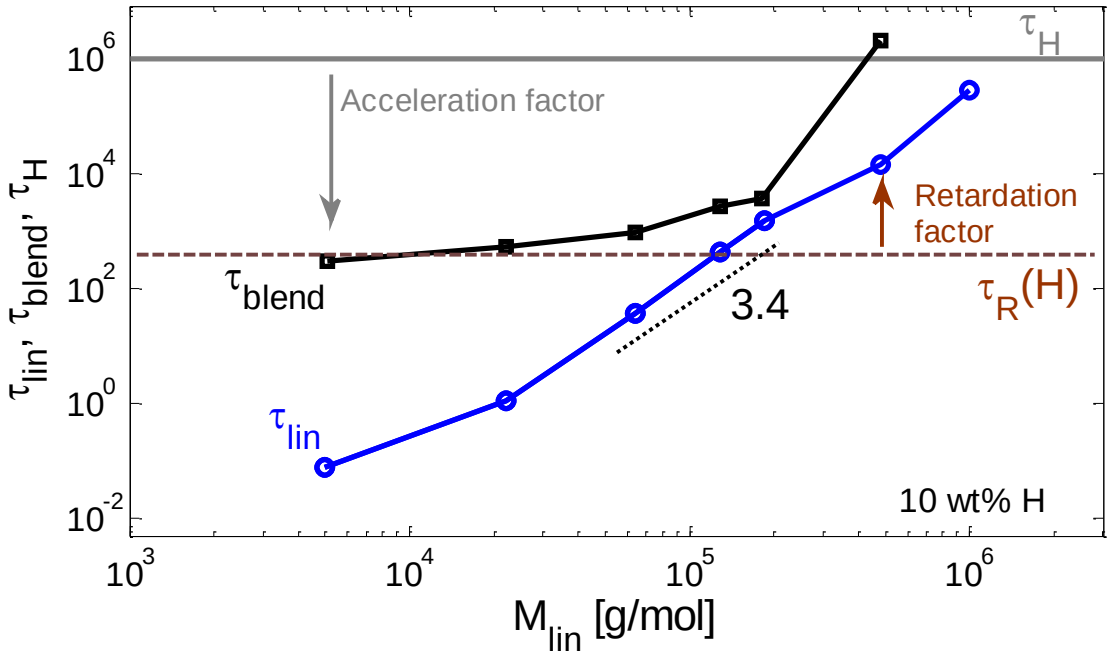

Figure 6. Comparison of the terminal relaxation time of blends with 10 wt% of H-PS, τ_{blend}, and that of the linear matrix, τ_{lin}, as function of the molar mass of the latter, M_{lin} at 130 ºC. The terminal time τ_H and Rouse time $\tau_R(H)$ of the monodisperse H-PS are indicated by horizontal full and dashed lines, respectively. The terminal times were determined experimentally by fitting the terminal regime with two lines of slopes 1 and 2 (for G" and G', respectively) and inverting the cross-over frequency. The only exceptions are the blends in the two largest molar masses linear matrices for which the terminal relaxation was too slow to be detected even by creep measurements. For the 483k matrix, the relaxation time was determined from the theoretical curves and involves some uncertainty. This was not attempted for the 1000k matrix because the uncertainty is huge (see also Figure 5).

If a longer linear matrix is used, such as PS 483k or PS1000k, one cannot easily discern the slow mode signalling the relaxation of the H-polymers, even with creep measurements. Indeed, at very low frequencies the onset of a slow mode is observed in the 483k matrix and only a hint is given

(small change in low-frequcny moduli slopes) for the 1000k (this is further discussed in Section V.4). Therefore, the relaxation time of the H polymer in the 483k matrix has been determined from the theoretical predictions, whereas for the case of 1000k matrix it is not reported due to larger uncertainty.

IV. Modeling analysis

In this Section we first briefly review the main features of the TMA model used for determining the viscoelastic properties of the monodisperse samples. This model has been presented in detail in ref. [14] for the linear matrix and ref. [7] for the H-samples. Then, based on the observations made in Section III, we propose a simple model to describe the relaxation of the H/linear blends.

IV.1 Time marching algorithm (TMA): The relaxation modulus of a polymer melt, G(t), is described by taking into account two different contributions:

$$G(t) = G_R(t) + G_d(t) \qquad (9)$$

The first contribution, $G_R(t)$, describes the high-frequency Rouse modes taking place at time scales shorter than the Rouse entanglement time τ_e, before the chains have time to experience the tube, as well as the longitudinal Rouse motion[4]:

$$G_R(t) = \sum_k \frac{\upsilon_k \rho RT}{M_k} \left\{ \frac{1}{4} \sum_{p=1}^{Z_k} exp\left(\frac{-p^2 t}{\tau_R(M_k)}\right) + \sum_{p=Z_k+1}^{n} exp\left(\frac{-2p^2 t}{\tau_R(M_k)}\right) \right\}, \qquad (10)$$

with υ_k and $\tau_R(M_k)$ representing the weight fraction and the Rouse time of the chain k, respectively (for monodisperse samples, k is fixed to 1). The second contribution, $G_d(t)$, describes the relaxation of the whole chains through disentanglement process (reptation, Contour Length Fluctuations (CLF)

and Constraint Release). It depends on both the unrelaxed fraction of initial tube segments, $\varphi'(t)$, and the dilation factor ϕ(t):

$$G_d(t) = G_N^0 \mu(t) = G_N^0 \varphi'(t) \{\phi(t)\}^{\alpha}. \quad (11)$$

The dilation factor $\phi(t)$ takes into account the effect of CR on the chain entanglements and defines the diameter of the dilated tube (such as $a = a_0 . \phi(t)^{-\alpha/2}$). It is a priori equal to the unrelaxed fraction of initial tube segments, $\varphi'(t)$. However, its decrease through time is limited by the fact that it cannot decrease faster than by a (Constraint Release) Rouse process. Since this condition does not apply to monodisperse samples, we don't consider it here.

On the other hand, the unrelaxed fraction of initial tube segments, $\varphi'(t)$, is determined by summing up the survival probabilities (by reptation or fluctuations) of at all molecular segments x_k of all the different chains k:

$$\varphi'(t) = \sum_k v_k \int_{x_k=0}^{x_k=1} p_{rept}(x_k, t)\, p_{fluc}(x_k, t)\, dx_k \quad (12)$$

As detailed in ref. [7], the probability $p_{rept}(x,t)$ of a segment x to survive from reptation process at time t is given by the Doi and Edwards equation[1], while the survival probability from fluctuation process is approximated by the decreasing exponential function, $exp(-t/\tau_{fluc}(x))$, where $\tau_{fluc}(x)$ is the fluctuations time corresponding to segment x.

It must be noted that in the case of unentangled chains (such as the linear matrix 5k and 22k), the polymer fully relaxes by Rouse process:

$$G_{lin}(t) = \frac{\rho RT}{M_L} \sum_{p=1}^{p=N} exp\left(\frac{-2p^2}{\tau_R(M_L)}\right) \quad (13)$$

When diluted in a very short chain matrix, the H-polymers can also relax by a Rouse relaxation. This is discussed in section IV.3.

Subsequently, the storage and loss moduli are determined from *G(t)* by using an approximation of Fourier transform, as proposed by Schwarzl.[75]. The material parameters of the model are the plateau modulus, G_N^0, the molar mass between two entanglements, M_e, and the Rouse time of an entanglement segment, τ_e. We consistently use the same best fit TMA parameters (M_e=14.8k, G_N^0 =230kPa, τ_e=0.5s and α=1) for all PS samples (linear and H) at a temperature of 130°C (or at iso-T_g condition for PS5, PS22 and PS1000k). These values are consistent with other works[64] when taking into account the horizontal and vertical shift factors associated with a temperature difference.

IV.2. Monodisperse H-polymer: The description of the relaxation of an H-polymer is more complex due to the hierarchical relaxation of its two generations of molecular segments (the branches and the inner part of the backbone). At timescales larger than τ_e, the polymer relaxation starts with the relaxation of the arms by early and activated fluctuations. After the arms retraction, the backbone segments are free to move and will proceed to relax by fluctuations modes[7]. A specificity of the TMA model, compared to other tube models[5,6], is to utilize a unique molecular coordinate system, from x=0 at the chain extremity to x=1 at the middle of the H-polymer (see cartoon in Figure 7a), in order to determine the fluctuation times of the inner backbone[7]. In such a way, continuity is ensured between the relaxation time of the last segment of the branches and the one of the first backbone segment. Within this reference system, the influence of branching chains is taken into account by considering an extra friction point in the fluctuations time of the molecular segments localized between the branching point $(x=x_{br})$ and $(x=1)$, as illustrated in Figure 7b. In the terminal regime, the reptation of the (entire) backbone will eventually take over as fluctuations will become exponentially slow.

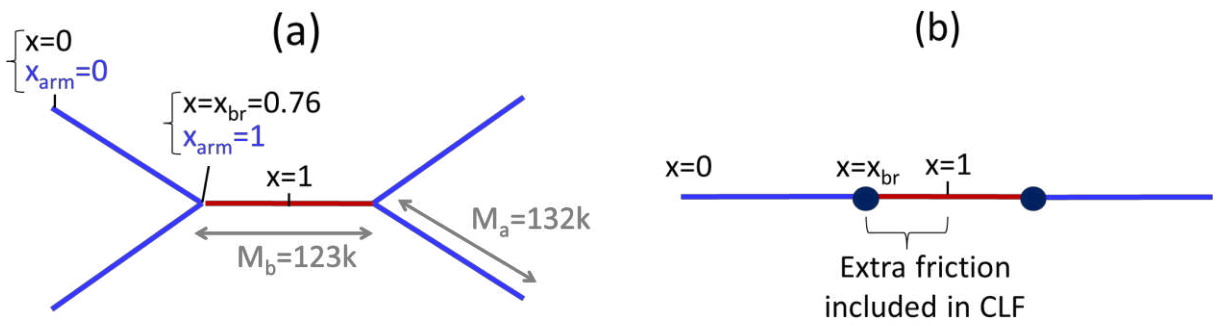

Figure 7: (a) H-polymer molecular coordinate systems. The first one, from the end of the branches, $x_{arm}=0$, to the branch point, $x_{arm}=1$, is used for determining the relaxation time of the molecular segments around the arms. The second one, from the end of the branches, x=0, to the middle of the backbone, x=1, is used to determine the relaxation time of the (inner) backbone. (b) At time longer than the relaxation time of the branches, these last ones are seen as extra friction points along the backbone of the H-polymer.

As discussed in refs. [57, 58], the presence of the branches has mainly two opposite effects on the relaxation of the inner backbone: on one hand, the motion of the branching points is strongly slowed down, which leads to extra friction felt by the backbone. However, on the other hand, it leads to large DTD effect due to the fast motion of the branches, which act as a solvent for the relaxation of the inner backbone[33]. This solvent effect is taken into account through the rescale of M_e in the calculation of the fluctuation times:

$$M_e(x) = \frac{M_{e,0}}{1-S(x)} , \qquad \text{for } x_{br} < x \leq 1 \tag{14}$$

with S(x), the relaxed fraction of the H-polymers, i.e. acting as a solvent, at the time the segment x is relaxing:

$$S(x) = \upsilon_{arm} + \upsilon_b \frac{x - x_{br}}{1 - x_{br}} \quad (15)$$

In equation 15, υ_b represents the weight fraction of the inner part of the H backbone. Alternatively, the backbone can relax by a Rouse relaxation process (if the volume fraction of the arms is large enough as to completely dilute the backbone, such as there is no backbone-backbone entanglement). In such a case, the monomeric friction from the branching points must also be taken into account.

IV.3. H-polymer diluted in an oligomeric linear matrix (M_{lin} = 5 kg/mol): Based on the experimental results (see Section III), we now propose a simple approach to describe the relaxation of the H-polymers diluted in a solvent-like (unentangled) matrix. This one is based on the fact that the H-polymers either do not contain self-entanglements (for the blends of H-polymers diluted at concentrations of 1.5 wt% and 3 wt%), or only contain 2.6 self-entanglements (for blends containing 10 wt% of H-polymers). Therefore, we can safely assume that the H-polymers are never confined in their 'dilated' tube, which only includes the H-H entanglements. Furthermore, the relaxation of the oligomeric linear matrix of mass 5kg/mol is so fast that it seems reasonable to consider it as acting as a real solvent. Therefore, the relaxation of the H-polymer in the 5 kg/mol matrix should be fully described by a Rouse relaxation.

Calculating the Rouse spectrum of branched polymer architectures is not trivial, and becomes more complicated as the degree of branching and asymmetry of the molecule is increased. In fact, for the special case of a symmetric H-Polymer it is possible to obtain the forms of the Rouse eigenmodes analytically, and so obtain simple equations that can be numerically solved to find the Rouse spectrum, as we detail in the Appendix. We suspect that a similar approach could be used (for example) for a Cayley tree architecture, but for molecules beyond that degree of symmetry it is likely that the only viable approach is numerical solution for eigenmodes of a Rouse connectivity matrix, as proposed in refs. [76-78] for star polymers. As an alternative, in the main body of the paper we detail an approximate approach based on the insight that at high frequencies all polymer

architectures have effectively the same Rouse relaxation spectrum (since at short timescales, Rouse relaxation involves the collective motion of short chain subsections, but is insensitive to the larger scale connectivity of the molecule). Only the longest Rouse modes, corresponding to collective motion of chain sections larger than the distance between branching points (or from branching point to chain end), are significantly affected by the molecular connectivity, and so give differences from one molecular architecture to another. We show in the Appendix that this approximate approach gives results very close to the exact calculation for an H-polymer. We consider that the approximate approach can be a useful starting point for application to more complex architectures and so focus on this in the main text.

In the approximate approach, the longest Rouse mode is attributed to the relaxation of the largest molecular segment, i.e., the largest end-to-end path between two chain extremities, of mass equal to 132+2x123=387 kg/mol. This span molar mass is called M_H hereafter. In such a way, we ensure keeping consistency with the Rouse relaxation of an H-polymer having two of its branches replaced by extremely small branches, thus nearly forming a linear chain of mass 387 kg/mol. In addition, the possible influence of the branching point on the Rouse motion of H-polymers must be taken into account. Here, we assume (as detailed above) that for Rouse modes involving chain subsections smaller than one branch or the inner backbone, the branching points should have no effect on the Rouse relaxation. Hence for fast relaxations we simply use the Rouse spectrum of linear chains of mass M_H. However, the slower motion and higher friction from side branches could potentially delay the longest Rouse modes, which involve molecular segments longer than M_a (132 kg/mol) or M_b (123 kg/mol). In the specific case of the H-PS studied here, we assume that these long modes correspond to the entire chain (mode 1) or to half of the chain (mode 2) from the Rouse spectrum of linear chains of mass M_H, as illustrated in Figure 8.

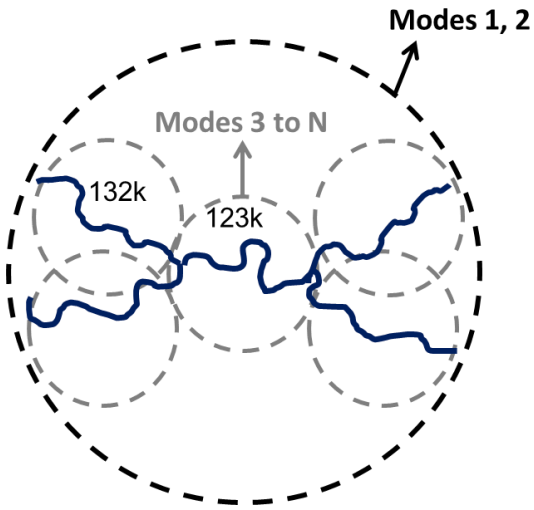

Figure 8: Description of the different Rouse modes present in the relaxation of unentangled H-polymer diluted in an oligomeric linear matrix. The grey circles define the longest molecular segment which can relax according to its intrinsic Rouse relaxation. The longest modes, 1 and 2, are possibly delayed by the slow motion of the branching points or self-entanglements.

Another potential source of delay, for the component of the relaxation modulus attributed to these two longest Rouse modes, is the few H-H entanglements, on average 2.6 per M_H, which are present when the H-polymer is diluted at 10 wt%. Since they would affect exactly the same Rouse modes as the branching points, it is not easy to separate these two contributions. However, they should only affect the blends containing 10% of H-polymers, while the delay due to branching point motion should be detected whatever the H-concentration may be. In order to take into account these two slower Rouse modes, we introduced a possible delay, θ_H, in their corresponding Rouse relaxation. The relaxation modulus can then be described, considering both the H-polymer and the unentangled matrix:

$$G(t) = G_H(t) + G_{lin}(t) \quad (16)$$

$$G_H(t) = \upsilon_H \frac{\rho RT}{M_H} \cdot \left(\sum_{p=3}^{N} exp\left(\frac{-2\,p^2 t}{\tau_{Rouse}(M_H)}\right) + \sum_{p=1}^{2} exp\left(\frac{-2\,p^2 t}{\theta_H \cdot \tau_{Rouse}(M_H)}\right) \right) \quad (17)$$

$$G_{lin}(t) = \upsilon_{lin}\frac{\rho RT}{M_{lin}} \cdot \left(\sum_{p=1}^{N} exp\left(\frac{-2\,p^2 t}{\tau_{Rouse}(M_{lin})}\right)\right) \quad (18)$$

with N, the number of Kuhn segments in the chain. In these equations, $\tau_{Rouse}(M_{lin}) = \tau_e Z_{lin}^2$ represents the Rouse time of the diluting linear chains, while $\tau_{Rouse}(M_H) = \tau_e Z_H^2$ represents the Rouse time of a linear chain of mass equal to span molar mass, M_H, i.e. without accounting for the possible influence of the branching points. Equation (17) is therefore just a modified Rouse spectrum for such a linear chain, with the longest two modes delayed by factor θ_H. The value of θ_H is not known and is determined in Section V, by best-fitting procedure on the viscoelastic data of this specific blend. While based on a single H-polymer one cannot investigate how this parameter depends on the H characteristics, it does not bring a large degree of freedom to the model since θ_H should not depend on the linear matrix as long as the H-polymers are relaxing by Rouse modes.

As noted above, in the Appendix we present an alternative to Equation (17) based on the exact solution of the Rouse model for the H-polymer architecture, comparing that result to Eq. (17).

IV.4. H-polymer diluted in a weakly entangled short linear matrix ($M_L \leq 185$ kg/mol): A priori, the H-polymers diluted in an entangled linear matrix can relax according to numerous different mechanisms. They can relax in their thin tube, if the entanglement with the linear matrix has too long a lifetime to be neglected. At later times they might be considered to relax in a dynamically dilating tube, as relaxation of the linear chains provides release of their entanglement constraints (if the H-polymers are sufficiently concentrated, entanglements between H-polymers would also need to be considered here). The process of enlarging the dynamically dilating tube is, in fact, the Constraint Release Rouse (CRR) process: the H-polymers are moving via Rouse motion in a sea of linear chains, at the rhythm of the destruction/re-construction of the entanglements involving the linear chains. Since the H3A1 samples diluted at 1.5, 3 or 10 wt% contain no or very few self-

entanglements (see Section IV.3), the CRR process on its own provides a mechanism to relax practically the whole of the stress carried by the H-polymers.

Based on the discussion in Section III (see Figure 4), it seems reasonable to consider that the relaxation time of the short linear matrix ($M_L \leq 185$ kg/mol) is well-separated from those of the monodisperse H-polymer. Given this, we may assume that the CRR process is the fastest mechanism of the ones discussed above and so dominates the relaxation of the H-polymers. We will proceed on the assumption that it is the only relaxation mechanism, i.e. assuming all relaxation takes place via CRR and neglecting relaxation via tube escape (from thin or dynamically dilating tubes). We may anticipate that this approximation is best for the shortest linear chains, but for longer linear chains, when CRR is slower, other relaxation mechanisms may become competitive.

It is important to note that while the H-polymer diluted in both an unentangled and an entangled matrix, are relaxing by Rouse, the two systems are quite different: the (Constraint Release) Rouse motion of the H-polymer in an entangled matrix is governed by the motion of the linear chains (i.e. by $\tau_{long\text{-}short}$ – see Equation 2), thus its terminal time can be much slower than in a oligomeric solvent. On the contrary, if the linear chains are too short to be entangled, the H-polymer relaxes according to its intrinsic Rouse process (i.e. governed by τ_e) rather than through CRR process. Therefore, as illustrated in Figure 9, Rouse modes of the H-polymer in an entangled matrix must be divided into three categories: i) the intrinsic Rouse modes of the molecular segments shorter than one entangled segment, which take place from the time ($t = \tau_0$) to ($t = \tau_e$); ii) The Rouse modes associated with molecular segments larger than M_e but which do not require the motion of the branching point, i.e. associated with molecular segments shorter than min{M_a (132 kg/mol), M_b (123 kg/mol)}, which must involve a delay factor, θ_{matrix}, in order to account for the influence of the slow motion of the linear chains; and iii) the longest modes (1-2), which are delayed by both the

linear matrix (θ_{matrix}) and the slow motion of the branching points and/or the H-H entanglements(θ_H).

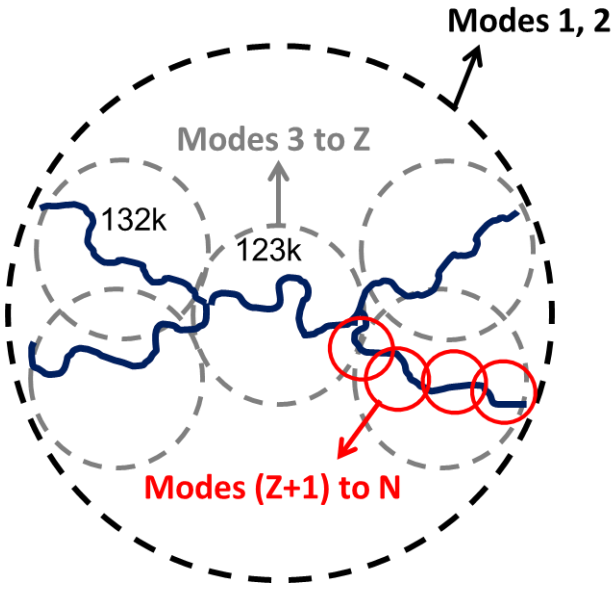

Figure 9: Description of the different Rouse modes present in the relaxation of H-polymer diluted in an entangled linear matrix. The red circles define the entanglement segments; the dashed grey circles define the longest molecular segment which can relax according to Constraint Release Rouse motion, at the rhythm of the motion of the linear chains. The dashed black circle describes the longest modes, 1 and 2, which are possibly delayed by both the linear matrix and the slow motion of the branching points and/or the few H-H entanglements.

From this scenario, we can determine the corresponding relaxation modulus, G(t). To do so, we use Equation (16) combined with the following expression for describing the H-polymer relaxation, which takes into account the possible delay in Rouse motion due to both the linear matrix (θ_{matrix}) and the branching point and/or the H-H entanglements (θ_H):

$$G_H(t) = \upsilon_H \left[\frac{\rho RT}{M_H} \cdot \left(\begin{array}{c} \sum_{p=Z_H+1}^{N} exp\left(\frac{-2\,p^2 t}{\tau_{Rouse}(M_H)}\right) + \sum_{3}^{Z_H} exp\left(\frac{-2\,p^2 t}{\theta_{matrix}.\tau_{Rouse}(M_H)}\right) \\ + \sum_{p=1}^{2} exp\left(\frac{-2\,p^2 t}{\theta_H.\theta_{matrix}.\tau_{Rouse}(M_H)}\right) \end{array} \right) \right] \quad (19)$$

with Z_H, the number of initial entanglement segment along the end-to-end span segment of mass M_H.

Furthermore, since the linear chains are entangled, their contribution to the relaxation modulus must include fast Rouse relaxation up to the entanglement segments, then their relaxation by CLF, reptation and CR:

$$G_{lin}(t) = \upsilon_{lin} \left[\frac{\rho RT}{M_{lin}} \cdot \left(\frac{1}{4} \sum_{p=1}^{Z_{lin}} exp\left(\frac{-p^2 t}{\tau_R(M_{lin})}\right) + \sum_{p=Z_{lin}}^{N} exp\left(\frac{-2\,p^2 t}{\tau_{Rouse}(M_{lin})}\right) \right) + \right.$$

$$\left. G_N{}^0 \cdot \varphi_{lin}{}'(t) . \left(\phi_{tube,lin}(t)\right)^{\alpha} \right] \quad (20)$$

In this equation, $\varphi_{lin}{}'(t)$ represents the unrelaxed fraction of initial tube segments of the linear matrix at time t, ranging from 1 at time ($t=0$) to 0 when the matrix is fully relaxed (since $G_{lin}(t)$ only focuses on the contribution from the linear chains), and $\phi_{tube,\,lin}(t)$ describes the diameter of the tube in which the linear chains are moving, in function of time. Since at this time scale, the H-polymer is still fully oriented, $\phi_{tube,\,lin}(t)$ is approximated as:

$$\phi_{tube,\,lin}(t) = \upsilon_H + \upsilon_{lin} \cdot \varphi_{lin}{}'(t) \quad (21)$$

Again, in these equations, a new parameter, θ_{matrix}, appears. Contrary to θ_H, this new parameter should vary as function of the molar mass of the linear chains since it represents the delay in the Rouse process of the H-polymer due to the slow motion of the linear matrix. However, if we assume that the relaxation time of the linear matrix is not influenced by the presence of the H-polymers, this parameter should not depend on the concentration of the latter. This assumption is valid here due to

the relatively low proportion of H-PS (from 1.5 wt% to 10wt%) and the rather fast relaxation of the linear chains (which occurs before DTD can influence their reptation process). As detailed in Section V, the parameter θ_{matrix} is first considered as a fit parameter, determining its value in order to correctly describe the loss and storage moduli of the blends. Then, these best-fit values are discussed and rationalized for the different blends.

V. Discussion

V.1. Viscoelastic relaxation of monodisperse samples: Before applying the model developed in Section IV to the H/linear blends, we first compare the linear viscoelastic data of the reference samples with the curve predicted by the TMA model, based on Section IV.1. Results are shown in Figure 10.

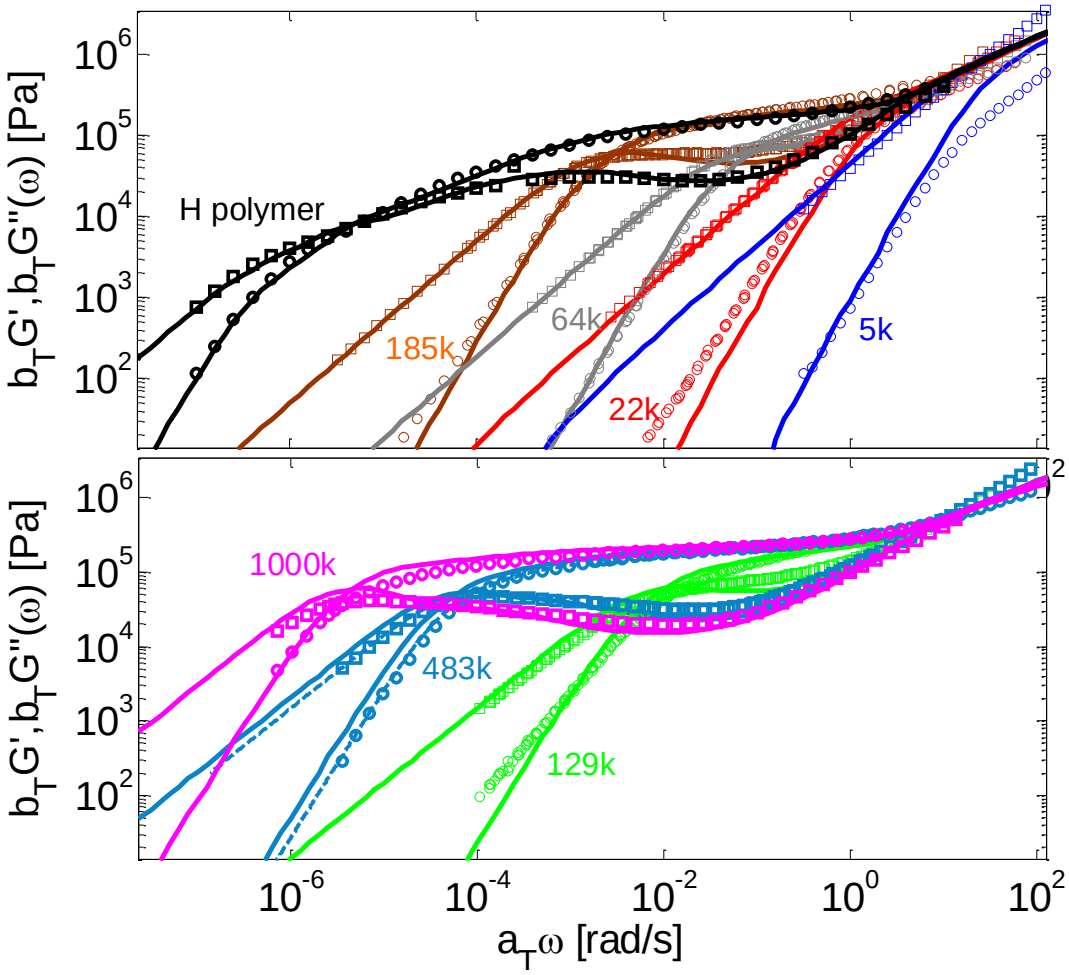

Figure 10: Experimental Storage (o) and loss (□) moduli of sample H3A1 H-polymer and of the linear matrices, at the master curve reference temperatures of 130°C. The continuous curves correspond to the data predicted with the TMA tube model (see Section IV.1). The dashed curves for samples 483k have been obtained from creep measurements.

While the overall agreement between the experimental and the theoretical curves is remarkable, a few comments are in order. First, we observe a large deviation between model predictions and data in the case of sample 5k at high frequencies. This suggests that, as already observed in [79] or in [80], in this frequency domain, the chains are not relaxing as described by a pure Rouse process. Second, the model does not exactly capture the behavior of the 22k matrix at low frequencies. This

is due to the very small number of entanglements, equal to 1.48 per chain. While PS 5k and PS 22k are considered as not entangled and monodisperse in the model, we cannot exclude the presence of a few longer chains containing some entanglements, which slightly slows down their relaxation. In addition, we observe that the model correctly describes the terminal relaxation of the H-polymer. In this case, the entangled branches are considered to relax by early and activated fluctuations (see Section IV.2). However, the way the inner part of the backbone is relaxing is not clear. If we consider that the relaxed branches act as a solvent after their relaxation, we find that the inner part of the backbone is not entangled anymore, while the whole backbone (i.e. the longest end-to-end molecular segment) still contains few entanglements and thus, relaxes by fluctuations or reptation, rather than by a Rouse process. While this is this last approach which has been followed in this work (consistently with ref. 7), one should note that both approaches lead to similar results. Given the limited data available, we cannot confirm the validity of either approach and leave this question open for future investigations.

V.2. Dilution of H-polymer in oligomeric linear chains: We next investigate the relaxation dynamics of a binary mixture consisting of 1.5 wt%, 3 wt% or 10 wt% of H-polymer (probe) diluted in oligomeric linear matrix, more specifically PS linear 5k (unentangled). The viscoelastic properties of this sample are modelled based on Equations (16-18) based on the Rouse model. As discussed in Section IV.2, the parameter θ_H is determined by best fitting procedure. As shown in Figure 11a, the experimental data of the blends containing only 1.5 or 3 wt% of H-polymer (in the unentangled state) are very well captured by considering θ_H =1. This means that the relaxation is well described by a Rouse process, and that the longest Rouse mode corresponds to the intrinsic Rouse relaxation of the longest end-to-end path between two chain extremities, i.e. the Rouse time of the H backbone in an oligomeric polystyrene at isofrictional condition. Thus, no specific delay coming from the branching points is observed, as we could have expected. The generality of this result is however not clear, since it is possible that the observed insensitivity of Rouse relaxation to the branching points

is due to the low number of branches attached to the polymer backbone in the specific case of a H-polymer. Furthermore, for these two blends, the relaxation of the H-polymers is independent of their weight fraction. This can be confirmed in Figure 11b, where the storage moduli of the three samples have been vertically shifted by a factor ($1/\upsilon_H$): it is observed that the relaxation peak of the samples containing 1.5 wt% and 3 wt% of H-polymer superimpose very well.

On the contrary, at 10 wt% in an oligomeric matrix, the H-polymer exhibits longer relaxation time (see Figure 11b). Whereas the good superposition of the shifted experimental data at intermediate frequency demonstrates that its relaxation mechanism has the same origin as those of the two other blends (i.e., it is well-described by a Rouse relaxation process), its longest (terminal) mode is longer. As shown in Figure 12, the latter is well captured if the value of θ_H is fixed to 2. As already mentioned, this larger value found with a 10 wt% concentration of H-polymer can be attributed to a delay of the longest relaxation modes due to the presence of a few entanglements (≈2.6) between the H-polymers. . In Figure 13, the influence of the delay of longest Rouse modes, can be observed by comparing the model predictions with θ_H = 1 (dotted curves) and θ_H = 2 (continuous curves). Hence, it can be concluded that the influence of this parameter is rather limited. While the value of θ_H =2 has been fixed here (by best-fitting process), the same value will be used for all blends composed of 10 wt% of H-polymer.

In order to get further insight about the sample relaxation, we analyze in the following the theoretical storage and loss moduli by considering the contribution of each component, i.e., the linear chains, and the H-polymer. From this decomposition, it is clear that the slow gradual decrease observed for G' at intermediate frequencies (10^{-2} rad/s to 1 rad/s) is due to the Rouse modes of the H-polymer, as observed with 1.5 or 3 wt% of H-polymer. Since the H-polymers are diluted in a 'solvent' matrix, this Rouse relaxation is intrinsic to them and therefore, could never become shorter even if a shorter linear matrix was used (while keeping constant $T-T_g$). This explains why the

signature of the H-polymer is so pronounced when it is blended into a very short linear matrix, where the ratio between their respective relaxation times, $\frac{\tau_{R,H}}{\tau_{R,L}}$, becomes larger with a shorter matrix.

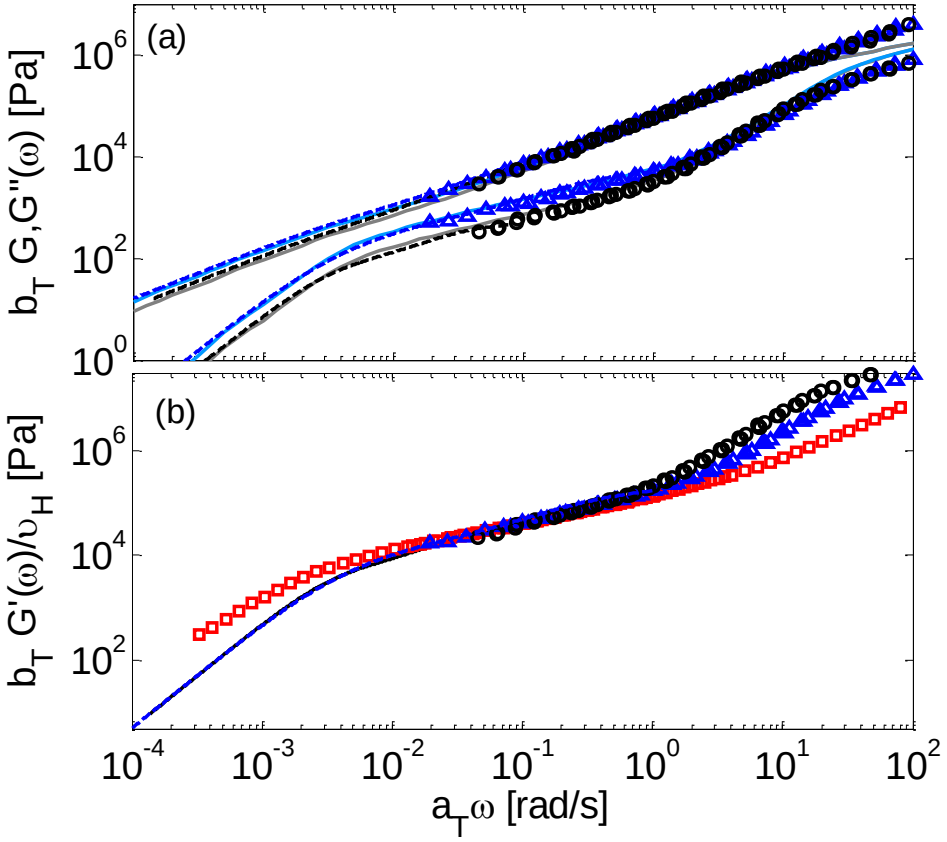

Figure 11: (a) Comparison between experimental (symbols and dashed curves) and theoretical (continuous curves) linear rheology data of 1.5 wt% (exp. data: black o and dashed curve (creep); predicted data: continuous grey curve) and 3 wt% (exp. data: blue Δ and dashed curve (creep); predicted data: continuous light blue curve) of H-polymer diluted in the PS5k linear matrix, at T_{ref} =130°C. The parameter θ_H has been fixed to 1. (b) Experimental storage modulus of 1.5 wt% (o), 3 wt% (Δ) and 10 wt% (□) of H-polymer diluted in the PS5k linear matrix, vertically shifted by dividing G'(ω) by the volume fraction of H-polymer, υ_H.

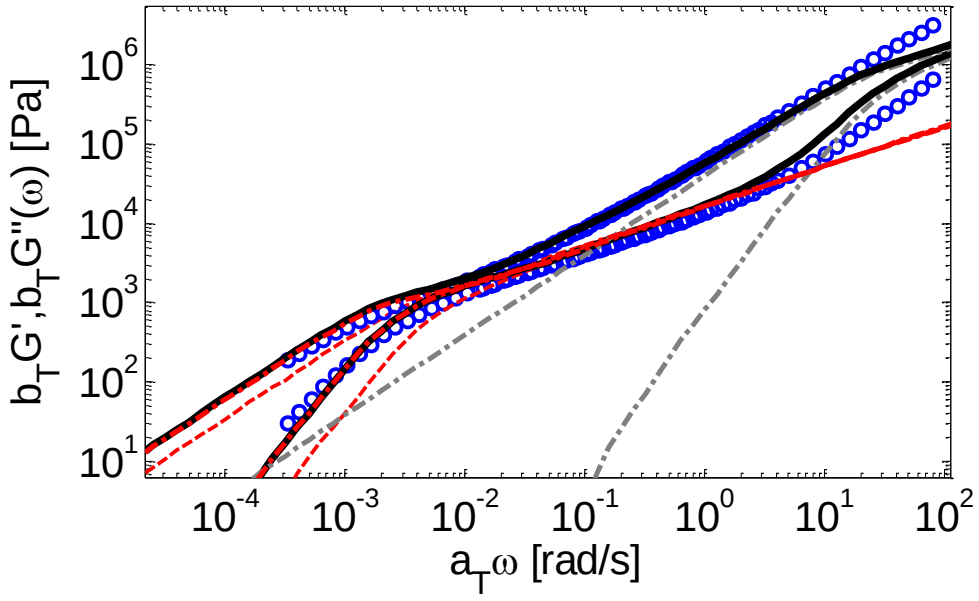

Figure 12: Comparison between experimental (o) and theoretical (continuous black curves) linear rheology data of 10 wt% of H-polymer diluted in the PS5k linear matrix, at T_{ref} =130°C. The parameter θ_H has been fixed to 2. The curves represent the contributions of the H-polymer (continuous red) and the linear matrix (dashed-dotted grey) to the moduli. The dashed red curves correspond to the predictions with $\theta_H = 1$.

Figures 11 and 12 also justify our choice to consider the longest end-to-end path on the H-polymer (the span molecular weight $M_H = M_b + 2M_a$) in order to define the longest Rouse mode (see Section IV.3). It should be noted that if the arms of the H-polymers were considered as fully relaxed at times longer than the Rouse time of molecular segments of mass M_a, 80 wt% of the H-polymers would have already relaxed at a frequency around 10^{-2} rad/s.

V.3. Dilution of H-polymer in short linear chains: As the molar mass of linear chains is increased above M_e, they no longer act as a solvent for the H-polymer, which is then expected to relax by Constraint Release Rouse (at the rhythm of the disentanglement/entanglement process of the linear chains) rather than by intrinsic Rouse relaxation. As described in Section IV.4., in our model, this is taken into account by considering the parameter θ_{matrix}, which represents the retardation factor between these two Rouse processes: $\theta_{matrix} = \frac{\tau_{CRR,H}}{\tau_{R,H}}$ (see Figure 6) and by using Equation (19) in order to model the relaxation of the H-polymers in the blends.

We first apply the model to blends with a barely entangled 22k linear matrix, which is considered to fully relax by Rouse motion (see Equation 18). However, since these linear chains are larger than M_e, even marginally, one cannot exclude that their presence slightly delays the relaxation of the H-polymers. In fact, this delay is confirmed in Figure 5, which shows that the relaxation time of the H-polymer is slightly longer in the 22k matrix compared to the 5k matrix. Since the value of θ_H is fixed to 2 for the blends with 10 wt% of H-polymer (see Section V.2), the value of the retardation factor θ_{matrix} is determined by a best-fitting procedure on the blend with 10 wt% H-PS in the 90 wt% 22k matrix (since it is the only unknown) with results shown in Figure 14. A value θ_{matrix} =1.5 is found, which represents a small delay effect of the barely entangled linear matrix on the motion of the H-polymer, confirming that in this case the latter relaxes as if the 22k matrix is nearly an oligomeric solvent. It is interesting to note that despite this small effect on the H-relaxation, the relaxation of the linear 22k matrix is much slower than that of the 5k matrix (see Figure 10). Therefore, the G' shoulder corresponding to the H-relaxation is much less pronounced in the 22k matrix than in the 5k matrix.

As mentioned in Section IV.4, the retardation factor θ_{matrix} should only depend on the molar mass of the linear matrix. Therefore, we use the same value for the two other blends, containing 1.5 and 3 wt% of H-polymers in the 22k matrix. As shown in Figure 13, in both cases a very good

agreement is obtained between model and experimental data when θ_H = 1. Hence, θ_H = 2 for all blends composed of 10 wt% of polymer, and θ_H = 1 for all blends composed of 3 or 1.5 wt% of H-polymer, conforming to the fact that the branching points have a negligible effect on the longest Rouse modes of the H-polymers considered here. On the contrary, the few H-H entanglements present at 10 wt% of H-polymer (≈2.6 on average) contribute to extra friction along the H-backbone, which delays its slower Rouse modes (1 and 2), involving molecular segments longer than the average molar mass between two H-H entanglements.

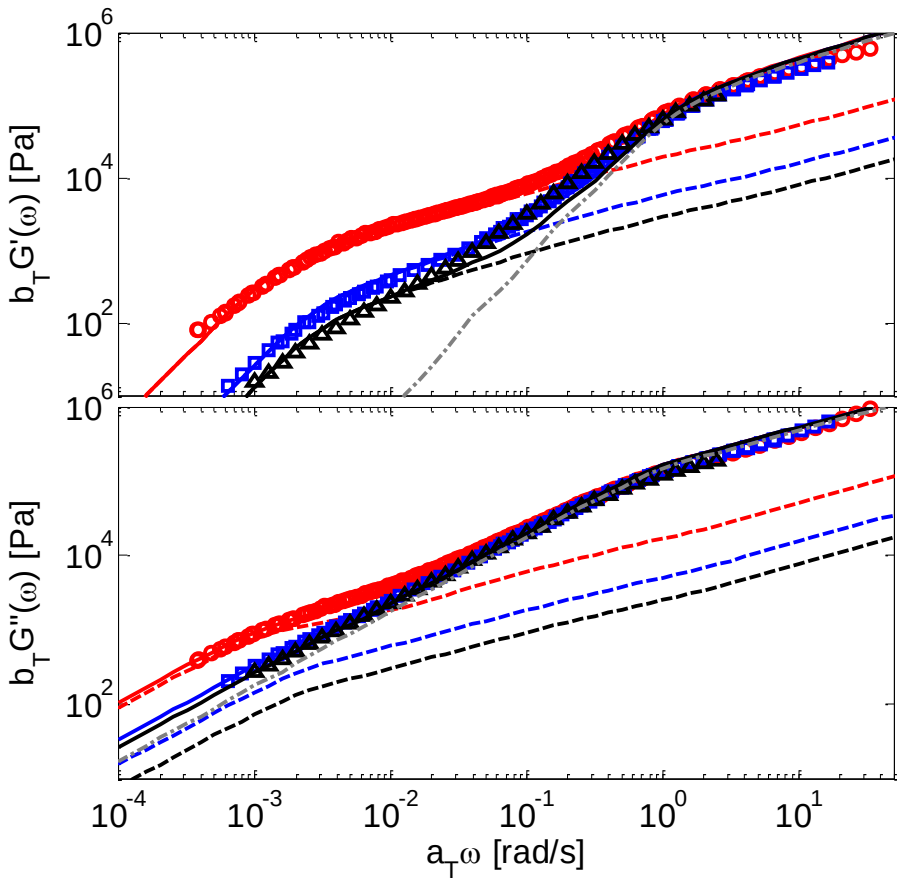

Figure 13: Storage G'(ω) and loss G''(ω) modulus data of 1.5% (Δ), 3%(□) and 10%(o) of H-polymer diluted in the linear matrix 22k, at T_{ref} =130°C. The experimental data (symbols) are plotted alongside the model data (continuous curves), as well as the deconvoluted linear (grey

dashed-dotted curves) and H (dashed curves) contributions to the curves. The parameter θ_{matrix} has been fixed to 1.5.

The same approach can be applied to the other blends. By increasing the molar mass of the linear matrix, the retardation factor θ_{matrix} is found to increase from 1.5 to 6, 19 and 58 for the matrices 22k, 64k, 129k and 185k, respectively, while θ_H has the same values as for the previous blends. As shown in Figure 14, the proposed model allows us to accurately describe the viscoelastic properties of these blends. This good agreement suggests that the H-polymers predominantly relax by a CRR process. This can be understood based on Figure 10, in which it is seen that even if these linear chains are well entangled, their relaxation time stays faster than the relaxation time of the branches of the H-polymers. By increasing the length of the linear matrix, it is expected that this difference in relaxation times decreases, until the point where the H-arms relax faster by fluctuations than by CRR at the rhythm of the linear chains motion.

In Figure 14, we also observe that the G' shoulder related to the relaxation of the H-polymers decreases substantially with increasing the molar mass of the linear matrix, and nearly disappears in matrix 185k, as discussed in Section 3.2. For this reason, we do not probe the full shape of the CRR relaxation spectrum of the H-polymers in the data, but rather only their terminal relaxation, and consequently it is impossible to rule out that other relaxation mechanisms, such as tube escape, contribute to the terminal relaxation process.

However, despite this small shoulder corresponding to the H-relaxation, the corresponding retardation factor θ_{matrix} is found to be much more important for the blends with higher molecular weight linear molecules. Hence, we conclude that the H-polymer relaxation is strongly slowed-down by the linear matrix (with potentially large consequences on the rheological properties).

In Figure 14, we separate the theoretical moduli of the 185k-blends into the contributions from the linear and the H-polymers. The moduli of the latter clearly show two Rouse relaxation processes: the first one, at high frequencies, corresponds to its segmental Rouse dynamics (see Equation 9), which is limited to the entanglement segments. Then, a plateau is observed in the storage modulus data. At this stage, the H-polymers are trapped in their thin tube and cannot relax further. At lower frequencies, we observe their CRR relaxation, which starts at a time equal to $\theta_{matrix}\tau_e$ and ends as soon as the longest mode (corresponding to the longest end-to-end molecular segment) is relaxed. As seen in this Figure, the theoretical result suggests that the CRR process of the H-polymers appears to start before the linear matrix is fully relaxed. Indeed, as already mentioned, if CRR was fully dominated by the matrix terminal relaxation time τ_{lin}, the G' shoulder corresponding to the H-relaxation should always be observed at the same frequency relative to the terminal relaxation frequency of the linear chains, which is obviously not the case. This can be explained by the fact that the H-polymers take time for exploring their dilated tube by CRR. Therefore, since their tube is not fully dilated when CRR starts, but is dilating fast enough to allow each CRR mode to relax, the H-polymers should never feel topological constraints from their surrounding tube. However, in order to validate this scenario, one should further analyze and rationalize the values used for the retardation factor θ_{matrix} in the different blends, as proposed in Section V.5. At this stage, we just note that similar results were found in ref. [31], where it was shown that the CRR process of the long component (star polymers in that case) starts at a time Z_{lin}^2 times shorter than the relaxation time of the linear matrix, τ_{lin}. Similar behavior was also observed by Read et al.[16] for moderately entangled linear matrices, based on slip-spring simulations (see Section V.5).

Furthermore, it is interesting to note that the model we propose here for describing the relaxation of the H-polymer at the rhythm of the relaxation of the linear matrix is very similar to the sticky Rouse model proposed by Colby[81] for describing the relaxation of unentangled linear chains

bearing stickers along their backbone. Indeed, for both types of systems the relaxation is governed by two Rouse dynamics: the first is associated to intrinsic Rouse motion taking place for molecular segments shorter than M_e (in the case of H/linear blends) or shorter than the average mass between two stickers (in the case of sticky chains), while the second reflects slower Rouse modes, dominated either by the long-short entanglements (in case of H/linear blends) or by the lifetime of the stickers (in the case of sticky chains). Only the delay θ_H induced by the few H-H entanglements along the H-backbone does not have any equivalent in the sticky Rouse model.

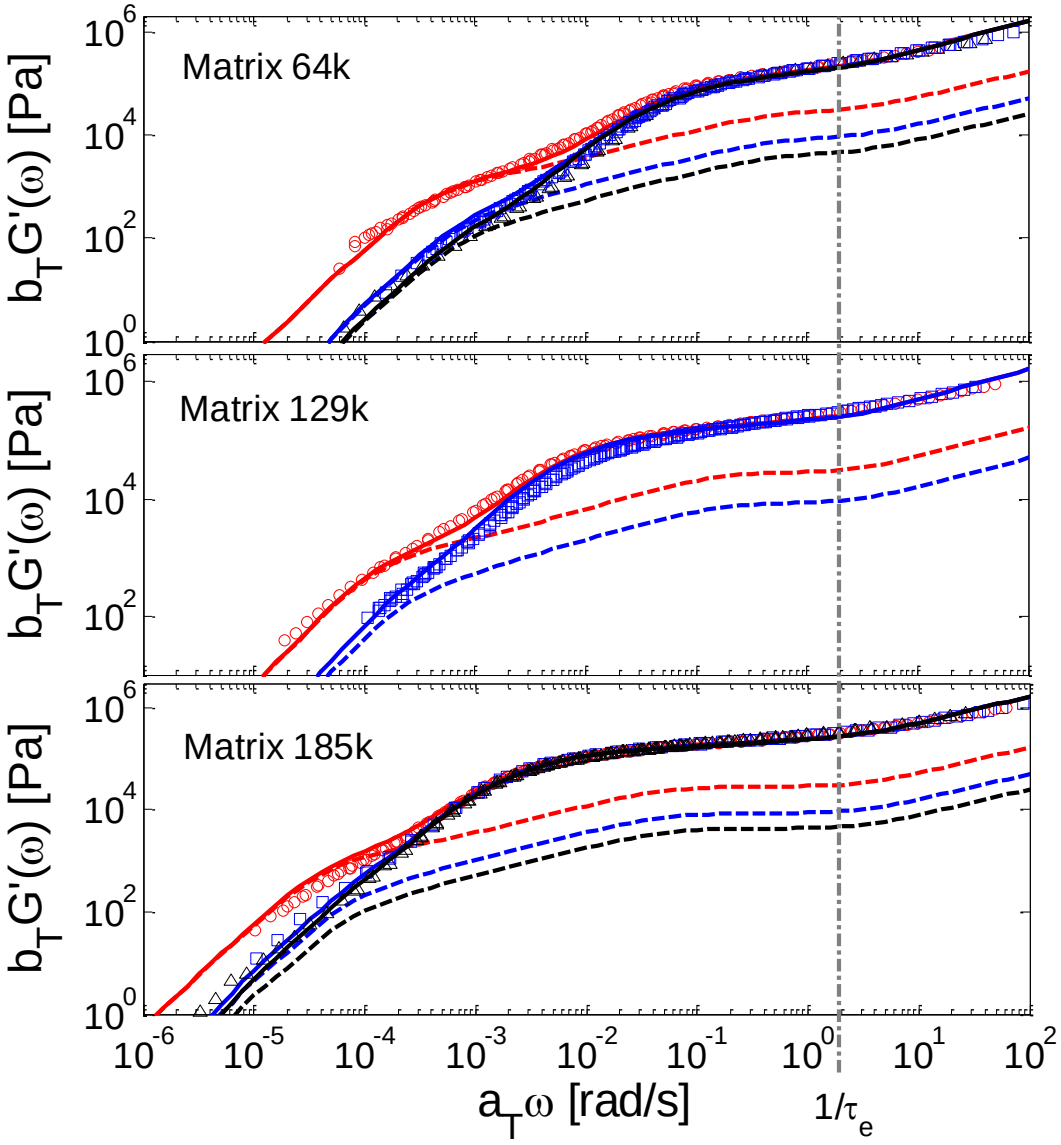

Figure 14: Storage G'(ω) and loss G''(ω) modulus data of 1.5% (Δ), 3%(□) and 10%(o) of H-polymer diluted in the linear matrices 64k, 129k and 185k, at T_{ref} = 130°C. The experimental data (symbols) are plotted alongside the model (continuous curves), as well as the H contribution (dashed curves). The retardation factor θ_{matrix} has been fixed to 6 (matrix 64k), 19 (matrix 129k) and 58 (matrix 185k).

V.4. Dilution of H-polymer in long entangled linear chains: Upon further increasing the molar mass of the linear matrix to 483 kg/mol or 1000 kg/mol, the large separation between the reptation time of the matrix and the relaxation of the H branches is lost (see Figure 4). Therefore, because of the long lifetime of their entanglements with the linear matrix, one cannot consider anymore that the H-polymers relax by a Rouse process and that the linear matrix acts as a solvent for the relaxation of the branches of the H molecules. However, since both the linear chains and the branches of the H molecules are relaxing much faster than the inner part of the backbone of the H-polymer, they are expected to play the role of an effective solvent for the remaining unrelaxed part of the inner H-polymers, enabling them to explore their surroundings. Thus, CR effects from the linear matrix and the H branches should speed-up the relaxation of the inner part of the H-polymers. We therefore model the relaxation of these blends by using Equations 10 and 11 and considering the retraction process of the inner backbone of the H-polymers in their tube, taking into account the extra friction coming from the branches (see Section IV.2) as well as the extra solvent coming from the linear matrix. Theoretical curves are compared to the experimental data in Figure 15, for the pure linear matrix as well as the blends composed of 10 wt% of H-polymer.

From the modeling results one may observe that the signature of the H-polymer is negligible at intermediate frequencies and only appears in the terminal flow region, when the storage modulus is lower than $G_N^0 v_b$, with v_b being the weight fraction of the inner part of the backbone. In this

region, an extra shoulder appears, which is more visible with the linear matrix PS 483k than with PS 1000k. The experimental data also reveal the onset of a slow relaxation shoulder in these blends (see Figures 5, 15 and 16), confirming the ultra-slow relaxation attributed to the H polymer. However, whereas this shoulder seems real, it can be sensitive to the creep conversion, which has been achieved based on the NLReg approach developed by Honerkamp et al.[71]. Indeed, with such an approach it is known that the data obtained in the first and last decades of the frequency window may lose accuracy. Hence, we refrain from further discussing these data at present. Figure 16 shows the experimental data of Figures 14 and 15 (10% H-polymer in matrices 185k, 483k and 1000k) plotted as $\eta''(\omega)=G'(\omega)/\omega$ against frequency. This representation captures the low-frequency response more sensitively and further supports the presence of a slow relaxation in 185k matrix (a), which however progressively becomes barely detectable as the molar mass increases to 483k (b) and 1000k (c). This prevents a more detailed quantitative analysis. To bring the slow mode within the experimentally accessible window, dilution with a small-molecule or oligomeric solvent would be the choice but this is beyond the scope of the present work. It is even worth noting that in this sensitive plot (the out of phase dynamic viscosity is in linear scale), even for the 185k for which the slow relaxation process of the H-polymer is probed unambiguously, its characteristic time is captured by the Rouse model with delayed modes whereas its intensity (value of η'') is overpredicted by a factor of 2 (Figure 16a). The discrepancies are larger for the larger molar mass matrices, predicted based on the tube model. These observations call for further improvements of the current analysis.

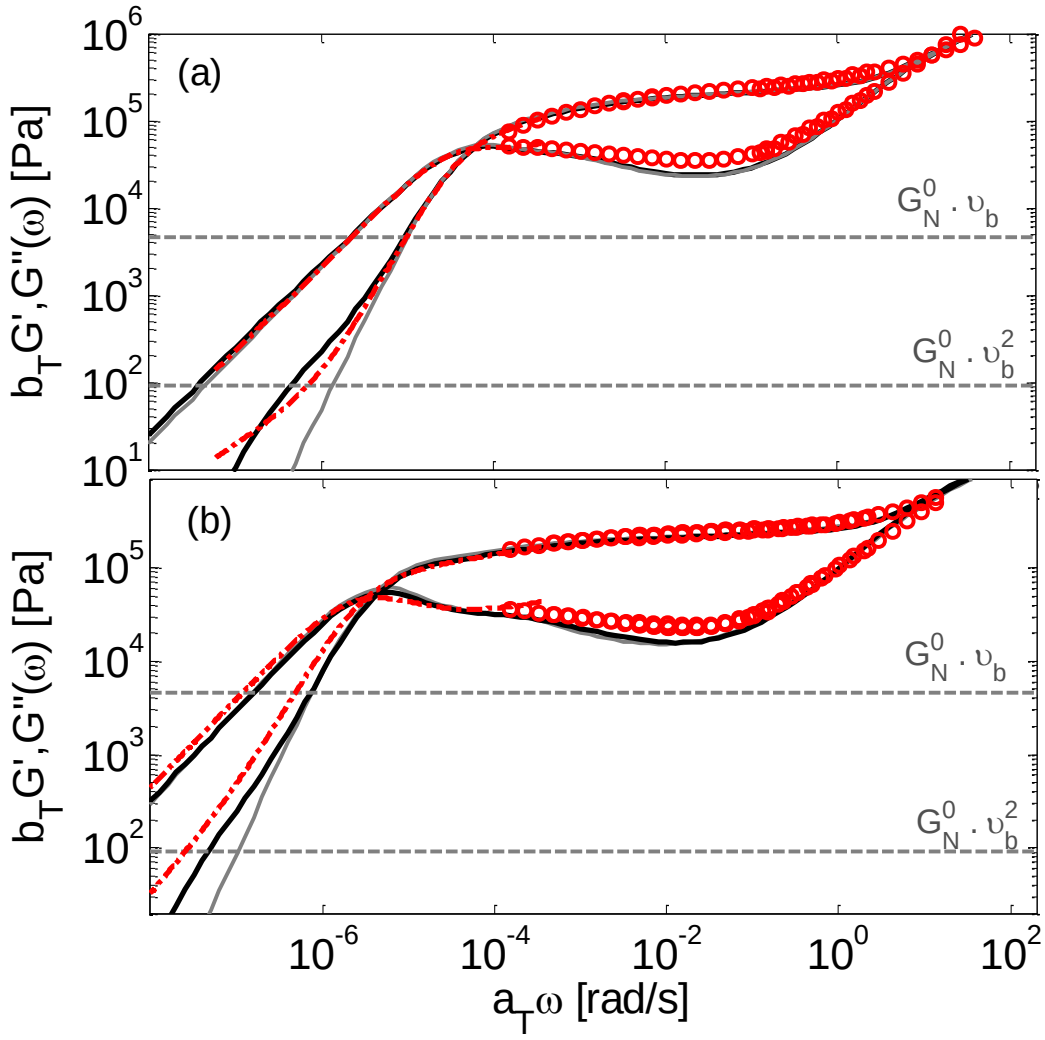

Figure 15: Comparison between experimental (red o and dashed curves for the data coming from creep measurements) and theoretical linear rheology data of 10 wt% of H-polymer diluted in linear matrices (continuous black curves) for (a) PS483k and (b) PS1000k For comparison, the predicted data obtained for the pure matrices are also shown (grey continuous curves).

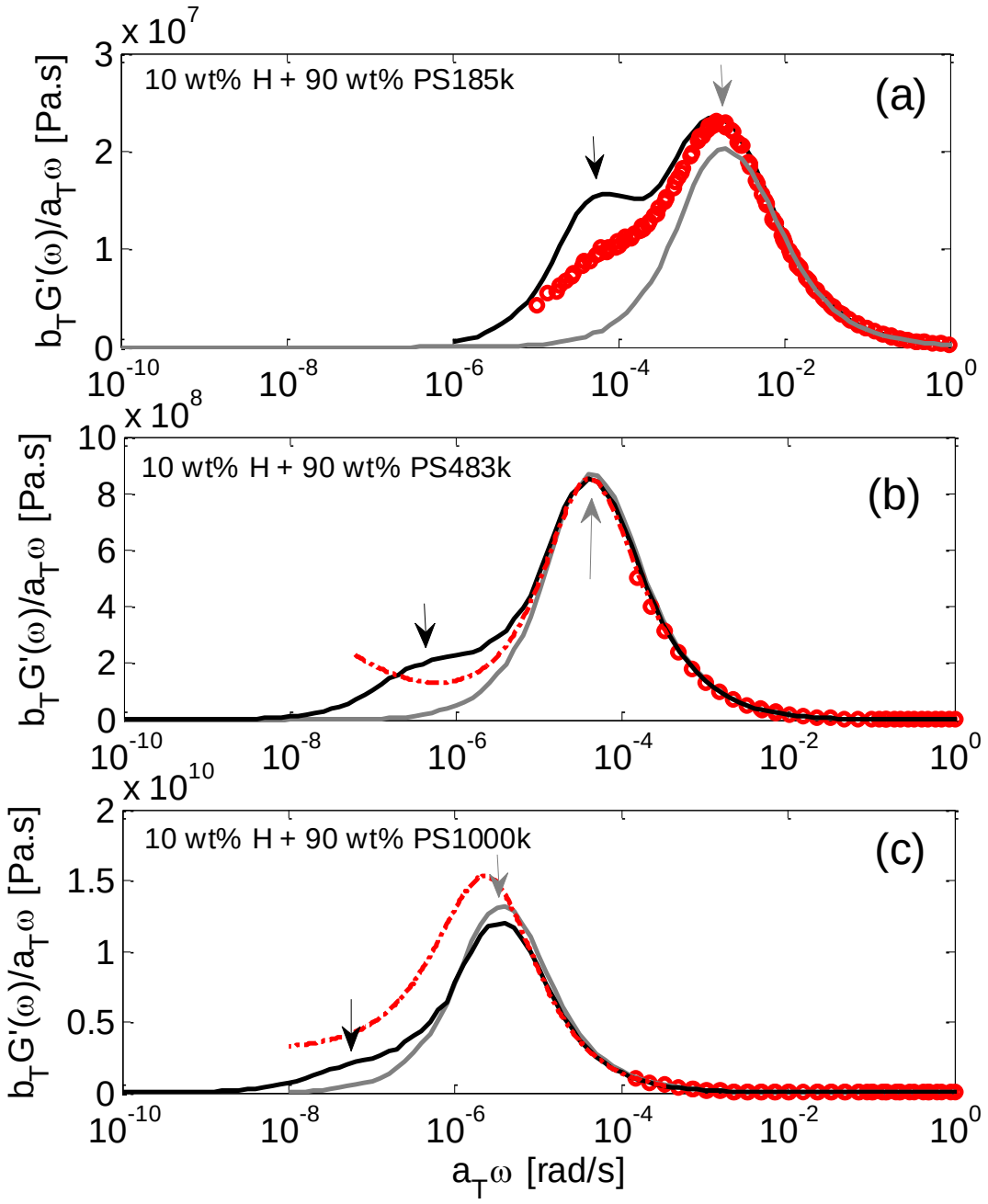

Figure 16: Same data as in Figures 14 and 15, but plotted as effective dynamic viscosity (G'(ω)/ω) against frequency. This representation sensitively captures the low-frequency region. Symbols are experimental SAOS data and dashed-dotted curves are transformed creep data of 10 wt% of H-polymer diluted in linear matrices comprising (a) PS185k , (b) PS483k and (c) PS1000k. The black lines are the theoretical predictions. The grey and black arrows indicate the theoretical relaxation

peaks of the matrix and the H polymer, respectively. For comparison, the predicted data obtained for the pure matrices are also shown (grey continuous curves).

V.5. Retardation factor θ_{matrix} for the relaxation of the H-polymer: Compared to its relaxation in a monodisperse environment, the relaxation of a H-polymer diluted in a linear matrix is much faster for fast linear chains (M<185K) (see Section V.3). Therefore, we can envisage an acceleration factor, defined as the ratio between the terminal relaxation times of the monodisperse H-polymer and the blends (as proposed in Figure 6). However, since in their terminal regime the H-polymers are not entangled anymore or contain too few entanglements to relax in a constraining tube, it seems more instructive to look at the retardation factor θ_{matrix} of these blends compared to the terminal time of the H-polymers diluted in a small-molecule solvent (or equivalently, in an oligomeric PS matrix). Within this scenario, we consider the retardation factor corresponding to the ratio between the CRR time and the intrinsic Rouse time of the H-polymers (see Figure 6):

$$\theta_{matrix} = \frac{\tau_{CRR,H}}{\tau_{R,H}} = \frac{\tau_{long-short} {Z_H}^2}{\tau_e {Z_H}^2} \qquad (22)$$

where the average lifetime $\tau_{long\text{-}short}$ governing the CRR process in unknown, and Z_H is the number of entanglements in the H backbone. As discussed in Section V.3, this time cannot be simply proportional to the relaxation time of the linear chains, τ_{lin}, as proposed by Struglinsky and Graessley[10], otherwise the importance of the G' shoulder would have been identical for all blends with the same concentration of H-polymer. The failure of this rule (i.e., $\tau_{long-short} \propto \tau_{lin}$) is illustrated in Figure 17, where the values of θ_{matrix} obtained by best fitting procedure on the different blends are compared to the relaxation time of the linear matrix, τ_{lin}, as function of the molar mass of the linear chains. Clearly, the retardation factor is not following the same trend as τ_{lin}. Indeed, while

for very short matrix its value can never become lower than 1 (which represents the intrinsic Rouse relaxation of the H-polymers in an oligomeric solvent at isofrictional condition), it does not increase as fast as the reptation time of the entangled matrix.

This conclusion is in good agreement with previous works[14,16-18,31]. In particular, in their recent paper[16], Read et al. determined this retardation factor, based on slip-spring simulations on bidisperse linear blends, and found that it is well estimated by:

$$\theta_{matrix}(slip-spring) = 0.047\,\frac{\tau_{lin}}{\tau_e}\left(1+\frac{1}{0.36}\sqrt{\frac{\tau_e}{0.047\,\tau_{lin}}}\right)+1. \qquad (23)$$

Thus, while the dependence of this factor on τ_{lin} is rather complex for moderately entangled linear matrices, in the limit of very well-entangled short matrix $\tau_{long-short}$ should be smaller than τ_{lin} by a factor 0.047. As shown in Figure 17, the theoretical factors are rather close to the values of θ_{matrix} determined experimentally, despite some deviation observed for the longest matrices, which can be due to different reasons (such as the estimation of τ_{lin}, the estimation of the constants in Eq. 23, or an increasing effect of other relaxation mechanisms of the H-polymers in the longer matrices).

The retardation factor can also be compared to the scaling proposed by Ebrahimi et al.[31] based on star polymers diluted in an entangled linear matrix, according to which the retardation factor is inversely proportional to Z_{lin}^2, the square of the number of entanglement segments in a linear chain. In this case the retardation factor should be well-described by $\theta_{matrix} = \frac{\tau_{long-short}}{\tau_e} = \frac{\frac{\tau_{lin}}{Z_{lin}^{\,2}}}{\tau_e}$ and should be equal to 1 with unentangled matrix. As observed in Figure 17, the agreement between this scaling and the value of θ_{matrix} obtained experimentally is also very good (the origin of the factor 3 found in the relationship between θ_{matrix} and τ_{lin} is not clear, but was also found in ref. [31]). This suggests that rather than being the relaxation time of the linear matrix, the parameter

$\tau_{long-short}$ should be seen as a kind of 'rescaled τ_e' which represents the relaxation time of a molecular segment of mass M_e obtained if the entire linear chains were relaxing Rouse-like with a relaxation time τ_{lin} (rather than their intrinsic Rouse time).

It is interesting to note here that while both theoretical approaches lead to comparable values of θ_{matrix} for the data analyzed in this work, large differences are expected to be found with longer matrices. Indeed, while Eq. 23 predicts that for very well entangled matrices, θ_{matrix} is a proportional to τ_{lin}, Ebrahimi et al. proposed a scaling going with τ_{lin}/Z_{lin}^2. Therefore, in order to experimentally test these two different scaling laws, one should design and measure the CRR behavior of very long linear chains moving in a long matrix (Z_{lin}>20).

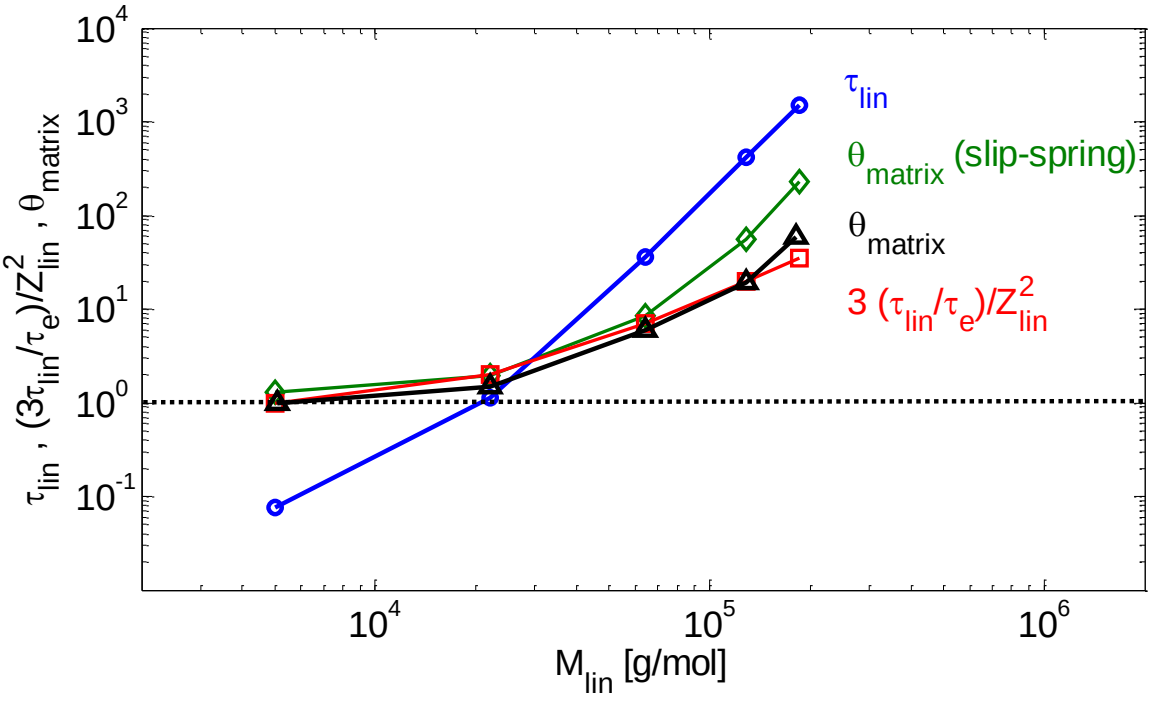

Figure 17: Retardation factor θ_{matrix}, θ_{matrix} (slip-spring), relaxation time of the linear matrix τ_{lin} and ratio $\frac{\frac{\tau_{lin}}{Z_{lin}^2}}{\tau_e}$ as functions of the molar mass of the linear matrix.

Note also that this definition of retardation factor is valid only if the long component is relaxing by CRR process. With longer linear matrices, such as 483k or 1000k, a significant part of the H-polymers is relaxing by fluctuations in their thin tube. Therefore, this relationship should not hold anymore.

VI. Conclusions

We investigated the role of constraint release on the relaxation of a model H-polymer diluted in a linear matrix of varying molar mass and concentration (1.5, 3 amd 10 wt % H). The experimental frequency spectra, obtained by dynamic oscillatory and complementary creep measurements, were analyzed by means of the TMA (Time-Marching Algorithm) model in order to quantitatively describe the linear viscoelasticity of the monodisperse component and validate the choice of the material parameters, i.e., the plateau modulus, the molar mass between two entanglements and the Rouse time of an entanglement segment. We then investigated the effects of the environment (molar mass of linear chain matrix) on the dynamics of the H-polymer. It was found that very short (oligomeric) linear chains act as a solvent, with the H-polymers relaxing according to their intrinsic Rouse modes. From these data, a time delay θ_H observed in the longest Rouse modes with 10wt% of H-polymers (corresponding to semidilute regime) was attributed to the presence of a few H-H entanglements inducing extra friction points to the Rouse relaxation.

As the molar mass of the linear chains increased, H-linear chain entanglements were formed. It was found that if the reptation time of the linear chains is faster than the retraction time of the branches, the linear chains also act as solvents for the H-polymers. However, the latter can only explore their dilated tube at the rhythm of the motion of the linear matrix. We took this into account by considering that the H-polymers relax according to a Constraint Release Rouse (CRR) process,

that we assumed to be slower than the corresponding intrinsic Rouse process by a factor θ_{matrix}. By analyzing the dependence of this retardation factor θ_{matrix} on the molar mass of the linear matrix, we showed that it is not only proportional to the relaxation time of the linear matrix, as usually considered[10], but also depends on the entanglement state (number of entanglements per chain) of the linear chains. This result is in agreement with the recent works of Read et al.[16] on bidisperse linear blends and Ebrahimi et al.[31] on star polymers diluted in a linear matrix, which suggests a generic picture of retardation factor of H-polymers in moderately entangled linear matrix environments. However, further analysis is needed in order to better understand the molecular origin of this non-proportionality between θ_{matrix} and τ_{lin}. Testing and potentially adjusting this picture in longer, well-entangled matrices is also an open challenge.

Acknowledgements

We thank J. Roovers and N. Hadjichristidis for generously providing the H- and linear-1000k polymer, respectively, used in this work. The DSC and SEC measurements were performed at the Max-Planck Institute for Polymer Research in Mainz, Germany. We acknowledge support by the EU (ITN DYNACOP 214627), NRF (SRC R11-2008-052-03002) and WCU (R31-2008-000-10059-0). EVR is chercheur qualifie of the FSR-FNRS.

A. Appendix: Exact Rouse modes of H-shaped architecture

In this Appendix we detail a solution for the exact Rouse modes of monodisperse H-shaped polymer in which all arms have identical molecular weight. The symmetry of the structure allows an exact determination of the mode structure. In general, for any linear section of chain within the branched

polymer, the equation of motion of the position **R** of a given monomer is identical to the standard Rouse model, i.e.

$$\zeta \frac{\partial \mathbf{R}}{\partial t} = k \frac{\partial^2 \mathbf{R}}{\partial n^2} + \boldsymbol{f} \tag{24}$$

where ζ is the monomer friction constant, $k = \frac{3k_BT}{b^2}$ is the monomer spring constant, n is a variable that counts monomers along the chain strand and $\boldsymbol{f}$ is the local stochastic force. Rouse modes of a polymer must be eigenmodes of the $\frac{\partial^2}{\partial n^2}$ operator along linear chain sections, i.e. along each linear chain section they must take the form:

$$\mathbf{R} = \mathbf{X}_p \left(A \cos \frac{p\pi n}{N} + B \sin \frac{p\pi n}{N} \right) \tag{25}$$

where $\mathbf{X}_p$ is the amplitude of the mode p and we have written the wavenumber as $\frac{p\pi}{N}$ (where N is the total degree of polymerisation) so that for a linear polymer p would take integer values to give the well-known Rouse modes of a linear chain. Substituting equation (25) back into (24) reveals that the relaxation time of mode p is:

$$\tau_p = \frac{N^2 b^2 \zeta}{3\pi^2 k_B T p^2} = \frac{\tau_R}{p^2} \tag{26}$$

where τ_R is the Rouse relaxation time of a linear molecule of degree of polymerisation N. For any given eigenmode of the chain, all linear chain subsections of the molecule must relax with the same timescale (they all have the same eigenvalue) and so all of them must take the same value p for the shape of the modes described in Equation 25 (i.e. the eigenmode has the same wavelength for every linear chain subsection). However, the form of the eigenmodes, and the allowed values of p (which in general will not be integers) are determined by the whole shape of the branched molecule and the boundary conditions at chain ends and branchpoints. An example of this calculation, for the symmetric star architecture, may be found in ref.[82]: here we generalise this to the H-shaped architecture. To do this we must specify the monomer coordinate frame we will use for each linear

chain subsection which we illustrated in Figure 18a. In terms of these co-ordinates, the boundary conditions are as follows. At chain ends of all four arms, there is no chain tension, hence:

$$\left.\frac{\partial \mathbf{R}_{A1}}{\partial n}\right|_{n=N_A} = \left.\frac{\partial \mathbf{R}_{A2}}{\partial n}\right|_{n=N_A} = \left.\frac{\partial \mathbf{R}_{A3}}{\partial n}\right|_{n=N_A} = \left.\frac{\partial \mathbf{R}_{A4}}{\partial n}\right|_{n=N_A} = \mathbf{0}. \quad (27)$$

At branchpoints, the displacements of all connected chains must be equal, so (for example) at the right hand branch-point:

$$\mathbf{R}_{A1}(n=0) = \mathbf{R}_{A2}(n=0) = \mathbf{R}_B\left(n = \frac{N_B}{2}\right). \quad (28)$$

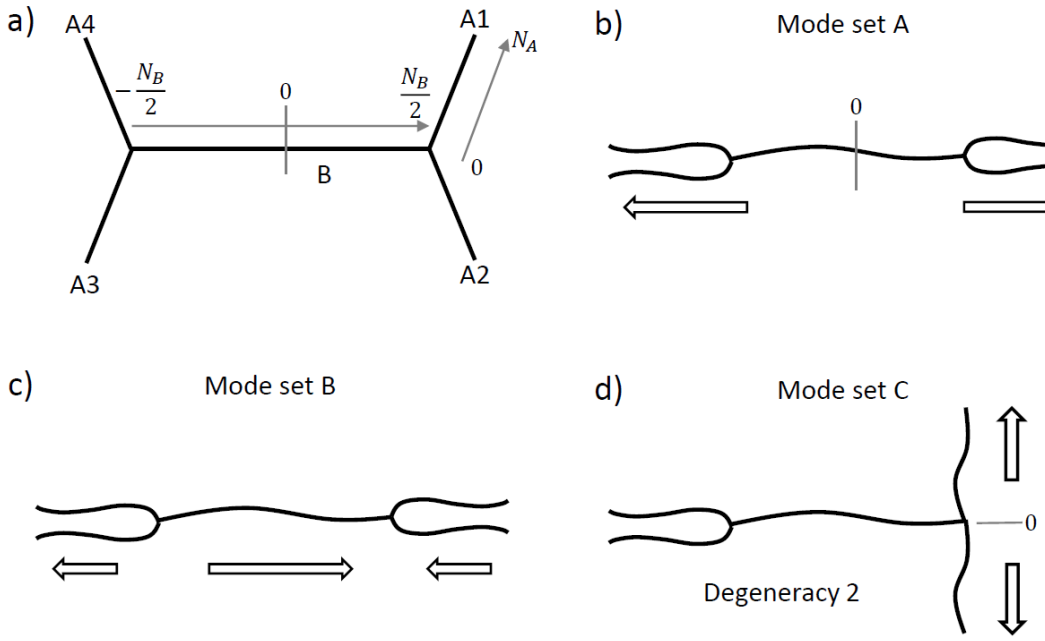

Figure 18: (a) Chain co-ordinates used for H-polymer modes. Backbone co-ordinate runs from $-\frac{N_B}{2}$ to $\frac{N_B}{2}$. Arm co-ordinates run from 0 (at branchpoint) to N_A. (b) Symmetry of Mode set A – asymmetric along molecule length with displacement node at centre of backbone. (c) Symmetry of Mode set B – symmetric along molecule length with displacement maximum at centre of backbone. (d) Symmetry of Mode set C – asymmetric along arms at one end of molecule with node at branchpoint and rest of molecule undisplaced. These modes have degeneracy 2. In all cases (Mode A, B and C) the slowest mode of the set is shown, but higher modes have the same symmetry.

Chain tension must also balance at the branchpoint, hence (again, for example) at the right-hand branchpoint:

$$\left.\frac{\partial \mathbf{R}_{A1}}{\partial n}\right|_{n=0} + \left.\frac{\partial \mathbf{R}_{A2}}{\partial n}\right|_{n=0} = \left.\frac{\partial \mathbf{R}_{B}}{\partial n}\right|_{n=\frac{N_B}{2}}. \quad (29)$$

Considering the symmetry of the H-molecule, we identify three mutually orthogonal sets of eigenmodes, depicted schematically in Figure 18(b-d). These are:

Mode set A: These are asymmetric along the length of the molecule, so:

$$\mathbf{R}_B = \mathbf{X}_p \sin\frac{p\pi n}{N} \quad (30)$$

and

$$\mathbf{R}_{A1}(n) = \mathbf{R}_{A2}(n) = -\mathbf{R}_{A3}(n) = -\mathbf{R}_{A4}(n) = \mathbf{X}_p\left(A\cos\frac{p\pi n}{N} + B\sin\frac{p\pi n}{N}\right). \quad (31)$$

Applying boundary conditions (28) and (29) at the branchpoint gives $A = \sin\frac{p\pi f_B}{2}$ and $B = \frac{1}{2}\cos\frac{p\pi f_B}{2}$ where $f_B = \frac{N_B}{N}$ is the backbone fraction. Then, applying boundary condition (27) gives:

$$2\sin\frac{p\pi f_B}{2}\sin p\pi f_A = \cos\frac{p\pi f_B}{2}\cos p\pi f_A \quad (32)$$

where $f_A = \frac{N_A}{N}$ is the arm fraction. Equation (32) can be solved to obtain the values of p for the Mode set A. For the H-polymer used in this paper ($f_B = 0.189$, $f_A = 0.203$) this yields p values {1.358, 5.000, 8.770, 11.518…}. Hence, the longest relaxation time of the molecule is $\frac{\tau_R}{1.358^2} = 0.543\tau_R$.

Mode set B: These are symmetric along the length of the molecule, so:

$$\mathbf{R}_B = \mathbf{X}_p \cos\frac{p\pi n}{N} \quad (33)$$

and

$$\mathbf{R}_{A1}(n) = \mathbf{R}_{A2}(n) = \mathbf{R}_{A3}(n) = \mathbf{R}_{A4}(n) = \mathbf{X}_p \left(A \cos \frac{p\pi n}{N} + B \sin \frac{p\pi n}{N} \right). \quad (34)$$

Applying boundary conditions (28) and (29) at the branchpoint gives $A = \cos \frac{p\pi f_B}{2}$ and $B = -\frac{1}{2} \sin \frac{p\pi f_B}{2}$. Then, applying boundary condition (27) gives:

$$2\cos \frac{p\pi f_B}{2} \sin p\pi f_A = -\sin \frac{p\pi f_B}{2} \cos p\pi f_A. \quad (35)$$

Equation (35) can be solved to obtain the values of p for the Mode set B. For the H-polymer used in this paper ($f_B = 0.189$, $f_A = 0.203$) this yields p values {3.710, 6.434, 10.000, 13.821…}, which are faster relaxations than for set A.

Mode set C: These comprise two degenerate sets of modes in which the backbone and the arms of one end do not move, while the arms at the other end stretch antisymmetrically from the branchpoint, which itself does not move. Hence one set of modes are given by:

$$\mathbf{R}_B = \mathbf{R}_{A3} = \mathbf{R}_{A4} = \mathbf{0} \quad (36)$$

and

$$\mathbf{R}_{A1}(n) = -\mathbf{R}_{A2}(n) = \mathbf{X}_p \sin \frac{p\pi n}{N}. \quad (37)$$

Boundary conditions (28) and (29) are automatically satisfied, whilst boundary condition (27) gives:

$$\cos p\pi f_A = 0 \quad (38)$$

with solutions $p = \frac{2m-1}{2f_A}$ for m =1,2,3… For the H-polymer used in this paper ($f_A = 0.203$) this yields p values {2.466, 2.466, 7.398, 7.398,…}, where the p values are repeated to indicate the degeneracy.

To obtain the linear viscoelastic spectrum, we note that each mode carries the same modulus contribution (equal to $k_B T$ times the number of molecules per unit volume, i.e. for H-polymers at fraction υ_H the modulus for each mode is $\upsilon_H \frac{\rho RT}{M_{\mathrm{H,total}}}$ where $M_{\mathrm{H,total}}$ is the total molecular weight of

the H-polymer. The stress relaxation time for each mode is one half the orientation relaxation time. Hence, the Rouse relaxation spectrum of the H-polymer (including only monomer friction) is then:

$$G_H(t) = \upsilon_H \frac{\rho RT}{M_{\mathrm{H,total}}} \sum_p \exp\left(\frac{-2\,p^2 t}{\tau_R}\right) \qquad (39)$$

where the summation is over all p values identified as solutions to equations (32), (35) and (38) above (with solutions to (38) repeated twice to account for the degeneracy of Mode set C). We list the numerical solutions for the first 50 modes in Table 4.

Although the spectrum of modes is not identical to that of a linear polymer of the same molecular weight (with p values now being non-integer in general) the modulus per mode is the same as for the linear polymer, and at high values of p the mode density is identical (i.e. one mode per unit increase in p on average). Hence at high frequencies (short times) the relaxation spectrum is identical to that of the linear polymer, as is expected because at these short times the Rouse modes correspond to local chain motion insensitive to the (rare) chain ends or branch points. This observation also acts as confirmation that Mode sets A, B and C above include all the available Rouse modes. However, the spectrum at the longest times, or lowest frequencies, does depend on the polymer architecture, so the shape of the relaxation curve changes in the approach to the terminal relaxation.

In Figure 19, the storage modulus predicted with this exact Rouse solution (see Eq. 16, 18 and 39) and the approximated Rouse model (see Eq. 16, 17 and 18) are compared in the case of 3 and 1.5 wt% of H polymer diluted in the oligomeric matrix of 5 kg/mol. As it can be seen, the difference between two approaches is very small. Only a slight difference appears at low frequency, where it seems that the longest modes of the exact Rouse model are slightly longer than the approximated model.

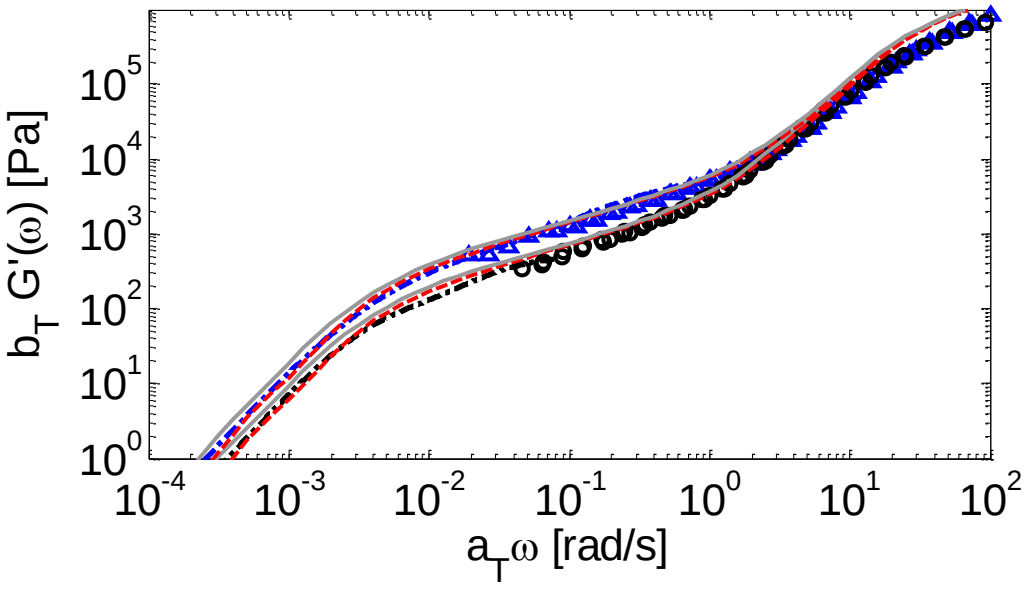

Figure 19: Comparison between experimental and theoretical linear rheology data of 1.5 wt% (exp. data: black o and dashed-dotted curve (creep)) and 3 wt% (exp. data: blue Δ and dashed-dotted curve (creep)) of H-polymer diluted in the PS5k linear matrix, at T_{ref} =130°C. The data predicted with the exact Rouse model are shown by the continuous grey curve, while the data predicted with the approximated Rouse model are shown by the dashed red curves.

Table 4: The first 50 p-modes for $f_B = 0.189$, $f_A = 0.203$

Mode set A (eq 31)	Mode set B (eq 34)	Mode set C (eq 37)
1.357668	3.710458	2.465909
5.000104	6.434078	7.397727
8.770082	10.00084	12.32955
11.51824	13.82128	17.26136
15.00284	16.60932	22.19318
18.86437	20.00676	27.12500
21.70621	23.89990	32.05682
25.01329	26.80758	36.98864
28.92852	30.02315	41.92045
31.91192	33.95098	46.85227
35.03709	37.01765	

38.96806	40.05587	NB Degeneracy of
42.12309	43.98055	above modes is 2
45.08030	47.22662	
48.98922	50.11114	

References

1. Doi, M.; Edwards, S. The theory of polymer dynamics, Oxford Univ. Press, New York, 1986.

2. Doi, M.; Graessley, W. W.; Helfand, E.; Pearson, D. S. Dynamics of polymers in polydisperse melts. Macromolecules 1987 20(8), 1900-1906.

3. de Gennes, P.G. Reptation of a polymer chain in the presence of fixed obstacles. The journal of chemical physics 1971, 55, 572.

4. Likhtman, A. E.; McLeish, T. C. B. Quantitative Theory for Linear Dynamics of Linear Entangled Polymers. Macromolecules 2002 35(16), 6332-6343.

5. Larson, R. G. Combinatorial rheology of branched polymer melts. Macromolecules 2001, 34(13), 4556-4571.

6. Das, C.; Inkson, N. J.; Read, D. J.; McLeish, T. C. B. Computational linear rheology of general branch-on-branch polymers. J. Rheol. 2006, 50, 207.

7. van Ruymbeke, E.; Bailly, C.; Keunings, R.; Vlassopoulos, D. A General Methodology to Predict the Linear Rheology of Branched Polymers. Macromolecules 2006 39(18), 6248-6259.

8. Rubinstein, M.; Colby, R.H. Self-consistent theory of polydisperse entangled polymers: Linear viscoelasticity of binary blends. The Journal of chemical physics 1988, 89, 8, 10.1063.

9. Watanabe, H; Kotaka, T. Viscoelastic properties and relaxation mechanisms of binary blends of narrow molecular weight distribution polystyrenes. Macromolecules 1984, 17, 2316-2325.

10. Struglinski, M.; Graessley, W.W. Effects of polydispersity on the linear viscoelastic properties of entangled polymers. 1. Experimental observations for binary mixtures of linear polybutadiene. Macromolecules1985, 18, 2630-2643.

11. Watanabe, H. Viscoelasticity and dynamics of entangled polymers. Progress in Polymer Science 1999, 24, 1253-1403.

12. van Ruymbeke, E.; Liu, C-Y.; Bailly, C. Quantitative tube model predictions for the linear viscoelasticity of linear polymers. Rheology Reviews 2007, 53–134.

13. van Ruymbeke, E.; Masubuchi, Y.; Watanabe, H. Effective value of the dynamic dilution exponent in bidisperse linear polymers: From 1 to 4/3. Macromolecules 2012, 45 (4), 2085-2098.

14. van Ruymbeke, E.; Shchetnikava, V.; Matsumiya, Y.; Watanabe, H. Dynamic dilution effect in binary blends of linear polymers with well-separated molecular weights. Macromolecules 2014, 47 (21), 7653-7665.

15. Read, D. J.; Jagannathan, K.; Sukumaran, S. K.; Auhl, D. A full-chain constitutive model for bidisperse blends of linear polymers. Journal of Rheology 2012, 56, 823.

16. Read, D. J.; Shivokhin, M. E.; Likhtman, A. E. Contour length fluctuations and constraint release in entangled polymers: Slip-spring simulations and their implications for binary blend rheology. Journal of Rheology 2018, 62, 1017.

17. Watanabe, H.; Ishida, S.; Matsumiya, Y.; Inoue, T. Viscoelastic and dielectric behavior of entangled blends of linear polyisoprenes having widely separated molecular weights: test of tube dilation picture. Macromolecules 2004, 37, 1937-1951.

18. Watanabe, H.; Ishida, S.; Matsumiya, Y. & Inoue, T. Test of full and partial tube dilation pictures in entangled blends of linear polyisoprenes. Macromolecules 2004, 37 (17); 6619-6631.

19. Watanabe, H.; Matsumiya, Y.; van Ruymbeke, E. Component Relaxation Times in Entangled Binary Blends of Linear Chains: Reptation/CLF along Partially or Fully Dilated Tube. Macromolecules 2013, 46, 9296-9312.

20. Park S.J., Larson R.G. Dilution exponent in the dynamic dilution theory for polymer melts. J. Rheol. 2003, 47, 199–211.

21. Park, S. J.; Larson, R. G. Tube Dilation and Reptation in Binary Blends of Monodisperse Linear Polymers. Macromolecules 2004, 37(2), 597-604.

22. Park, S. J.; Larson, R. G. Long-chain dynamics in binary blends of monodisperse linear polymers. Journal of Rheology 2006, 50(1), 21-39.

23. Liu, C.-Y.; Halasa, A. F.; Keunings, R. & Bailly, C. Probe Rheology: A Simple Method to Test Tube Motion. Macromolecules 2006, 39(21), 7415-7424.

24. Blottière, B.; McLeish, T. C. B.; Hakiki, A.; Young, R. N.; Milner, S. T. Rheology and Tube Model Theory of Bimodal Blends of Star Polymer Melts. Macromolecules 1998, 31(26), 9295-9304.

25. Struglinski, M; Graessley, W.W.; Fetters, L.J. Effects of polydispersity on the linear viscoelastic properties of entangled polymers. 1. Experimental observations for binary mixtures of linear and star polybutadiene. Macromolecules 1988, 21, 783-789.

26. Watanabe, H.; Yoshida, H.; Kotaka, T. Entanglement in blends of monodisperse star and linear polystyrenes. 1. Dilute blends. Macromolecules 1988, 21 (7), 2175-2183.

27. Milner, S. T.; McLeish, T. C. B.; Young, R. N.; Hakiki, A.; Johnson, J. M. Dynamic Dilution, Constraint-Release, and Star-Linear Blends. Macromolecules 1998, 31(26), 9345-935.

28. Milner, S. T. & McLeish, T. C. B. Reptation and contour-length fluctuations in melts of linear polymers. Physical Review Letters 1998, 81, 725–728.

29. Lee, J.H.; Archer, L.A. Stress relaxation of star/linear polymer blends. Macromolecules 2002, 35 (17), 6687-6696.

30. van Ruymbeke, E.; Coppola, S.; Balacca, L.; Righi, S.; Vlassopoulos, D. Decoding the viscoelastic response of polydisperse star/linear polymer blends. Journal of Rheology 2010, 54(3), 507-538.

31. Ebrahimi, T.; Taghipour, H.; Grießl, D.; Mehrkhodavandi, P.; Hatzikiriakos, P.G.; van Ruymbeke, E. Binary blends of entangled star and linear poly(hydroxybutyrate): Effect of constraint release and dynamic tube dilation. Macromolecules 2017, 50, 2535–2546.

32. Shivokhin, M. E.; van Ruymbeke, E.; Bailly, C.; Kouloumasis, D.; Hadjichristidis, N.; Likhtman, A.E. Understanding constraint release in star/linear polymer blends. Macromolecules 2014, 47, 2451–2463.

33. Watanabe, H.; Matsumiya, Y.; van Ruymbeke, E.; Vlassopoulos, D.; Hadjichristidis, N. Viscoelastic and Dielectric Relaxation of a Cayley-Tree-Type Polyisoprene: Test of Molecular Picture of Dynamic Tube Dilation. Macromolecules 2008, 41, 6110-6124.

34. Groves, D. J.; McLeish, T.C.B.; Ward, N.J.; Johnson, A.F. The blend rheology of some linear and branched polymers. Polymer 1998, 39, 16, 3877-3881.

35. Kapnistos, M.; Lang, M.; Vlassopoulos, D.; Pyckhout-Hintzen, W.; Richter, D.; Cho, D.; Chang, T.; Rubinstein, M. Unexpected power-law stress relaxation of entangled ring polymers. Nat Mater. 2008, 7(12), 997-1002.

36. McLeish, T. C. B.; Allgaier, J.; Bick, D. K.; Bishko, G.; Biswas, P.; Blackwell, R.; Blottière, B.; Clarke, N.; Gibbs, B.; Groves, D. J.; Hakiki, A.; Heenan, R. K.; Johnson, J. M.; Kant, R.; Read, D. J.; Young, R. N. Dynamics of Entangled H-Polymers: Theory, Rheology, and Neutron-Scattering. Macromolecules 1999, 32(20), 6734-6758.

37. McLeish, T.C.B. Tube theory of entangled polymer dynamics. Advances in physics 2002, Taylor & Francis, 1379-1527.

38. Tsenoglou, C. Molecular weight polydispersity effects on the viscoelasticity of entangled linear polymers. Macromolecules 1991, 24, 8, 1762-1767.

39. des Cloizeaux, J. Double reptation vs. Simple reptation in polymer melts. Europhysics Letters 1988, 5, 5.

40. Graessley, W. Entangled linear, branched and network polymer systems- Molecular Theories. Synthesis and Degradation Rheology and Extrusion. Springer Berlin Heidelberg 1982, 47, 67-117.

41. Marrucci, G. Relaxation by reptation and tube enlargement: A model for polydisperse polymers. Journal of Polymer Science, 1985, 23(1), 159-177.

42. Ball, R. C.; McLeish, T. C. B. Dynamic dilution and the viscosity of star-polymer melts. Macromolecules 1989, 22(4), 1911-1913.

43. Milner, S.T. and McLeish, T.C.B. Parameter-free theory for stress relaxation in star polymer melts. Macromolecules 1997, 30(7), 2159-2166.

44. Matsumiya, Y.; Kumazawa, K.; Nagao, M., Urakawa, O.; Watanabe, H. Dielectric Relaxation of Monodisperse Linear Polyisoprene: Contribution of Constraint Release. Macromolecules 2013, 46, 6067-6080.

45. Matsumiya, Y; Masubuchi, Y.; Inoue, T.; Urakawa, O.;,Liu, C.Y.; van Ruymbeke, E.; Watanabe, H. Dielectric and Viscoelastic Behavior of Star-Branched Polyisoprene: Two Coarse-Grained Length Scales in Dynamic Tube Dilation. Macromolecules 2014, 47 (21), 7637-7652.

46. Green, P.F.; Mills, P.J.; Palmstrom, C.J.; Mayer, J. W; Kramer, E. J. Limit of Reptation in Polymer Melts. Phys. Rev. Lett. 1984, 53, 2145.

47. Green, P.F.; Kramer, E.J. Matrix effects on the diffusion of long polymer chains. Macromolecules 1986, 19, 4, 1108-1114.

48. Green, P.F.; Palmstrom, C.J.; Mayer, J. W; Kramer, E. J. Marker displacement measurements of polymer-polymer interdiffusion. Macromolecules 1985, 18, 501.

49. Viovy, J. L.; Rubinstein, M.; Colby, R. H. Constraint release in polymer melts: tube reorganization versus tube dilation. Macromolecules 1991, 24, 3587-3596

50. Kan, H.-C.; Ferry, J. D.; Fetters, L. J. Rubber Networks Containing Unattached Macromolecules. 5. Stress Relaxation in Styrene-Butadiene-Styrene Block Copolymer with Unattached Linear and Star Polybutadienes, Macromolecules 1980, 13(6), 1571-1577.

51. Glomann, T.; Schneider, G. J.; Bras, A. R.; Pyckhout-Hintzen, W.; Wischnewski, A.; Zorn, R.; Allgaier, J.; Richter, D. Unified Description of the Viscoelastic and Dielectric Global Chain Motion in Terms of the Tube Theory. Macromolecules 2011, 44(18), 7430-7437.

52. van Ruymbeke, E.; Nielsen, J.; Hassager, O. Linear and nonlinear viscoelastic properties of bidisperse linear polymers: Mixing law and tube pressure effect. Journal of Rheology 2010, 54, 1155.

53. Shahid, T.; Huang, Q.; Oosterlinck, F.; Clasen, C.; van Ruymbeke, E. Dynamic dilution exponent in monodisperse entangled polymer solutions. Soft matter 2017, 13(1), 269-282.

54. Park S.J.; Larson R.G. Dilution exponent in the dynamic dilution theory for polymer melts. Journal of Rheology 2003, 47, 199–211.

55. Roovers, J.; Toporowski, P.M. Preparation and characterization of H-shaped polystyrene. Macromolecules 1981, 14, 5, 1174-1178.

56. Snijkers, F.; Vlassopoulos, D. Appraisal of the Cox-Merz rule for well-characterized entangled linear and branched polymers. Rheologica Acta 2014, 53, 12; 935-946.

57. Ahmadi, M.; Pioge, S.; Fustin, C.A.; Gohy, J.F.; van Ruymbeke, E. Closer insight in the structure of moderate to densely branched comb polymers by combining modeling and linear rheological measurements. Soft Matter 2017, 13, 1063-1073.

58. Kirkwood, K. M.; Leal, L. G.;Vlassopoulos, D.; Driva, P.; Hadjichristidis, N. Stress Relaxation of Comb Polymers with Short Branches. Macromolecules 2009, 42(24), 9592-9608.

59. van Ruymbeke, E.; Kapnistos, M.; Vlassopoulos, D.; Huang, T.; Knauss, D.M. Linear melt rheology of pompom polystyrenes with unentangled branches. Macromolecules 2007, 40, 5, 1713-1719.

60. Chang, T. Polymer characterization by interaction chromatography. J. Polym. Sci.: Part B: Polymer Physics 2005, 43, 1591.

61. Ryu, J.; Chang, T. Thermodynamic prediction of polymer retention in temperature-programmed HPLC. Anal. Chem. 2005, 77, 6347.

62. van Ruymbeke, E.; Lee, H.; Chang, T.; Nikopoulou, A.; Hadjichirstidis, N.; Snijkers, F.; Vlassopoulos, D. Molecular rheology of branched polymers: decoding and exploring the role of architectural dispersity through a synergy of anionic synthesis, interaction chromatography, rheometry and modelling. Soft Matter 2014, 10, 27, 4762-4777.

63. Fetters, L.J.; Lohse, D. J.; Colby, R. H. Chain dimensions and entanglement spacing. Physical Properties of Polymers Handbook, 2007, 447-454.

64. Shchetnikava, V.; Slot, J.J.M.; van Ruymbeke, E. A comparison of tube model predictions of the linear viscoelastic behavior of symmetric star polymer melts. Macromolecules 2014, 47, 3350–3361.

65. Larson, R. G.; Sridhar, T.; Leal, L. G.; McKinley, G. H.; Likhtman, A. E.; McLeish, T. C. B. Definitions of entanglement spacing and time constants in the tube model. Journal of Rheology 2003, 47, 809.

66. Liu, C.-Y. ; He, J. ; van Ruymbeke, E.; Keunings, R. ; Bailly, C. Evaluation of different methods for the determination of the plateau modulus and the entanglement molecular weight. Polymer 2006, 47, 4461-4479.

67. Ferry, J. D. Viscoelastic Properties of Polymers. Wiley, New York, 1980.

68. Dealy, J.; Plazek, D. Time-Temperature Superposition - A User's guide. Rheology Bulletin 2009,

78 (2).

69. Kapnistos, M.; Vlassopoulos, D.; Roovers, J.; Leal, L. G. Linear Rheology of Architecturally Complex Macromolecules: Comb Polymers with Linear Backbones. Macromolecules 2005, 38(18), 7852-7862.

70. Zoller, P.; Walsh, D. Standard Pressure-Volume-Temperature Data for Polymers; Technomic Publishing Co., New York, 1995.

71. Honerkamp, J.; Weese, J. A Nonlinear Regularization Method for the Calculation of Relaxation Spectra. Rheologica Acta 1993, 32 (1), 65−73.

72. Rubinstein, M.; Colby, R. H. Polymer Physics. Oxford University Press, 2003.

73. Fox, T.G.; Flory, P.J. Second-order transition temperatures and related properties of polystyrene. J. Appl. Phys. 1950, 21, 581–591.

74. Fox, T. G. Influence of Diluent and of Copolymer Composition on the Glass Temperature of a Polymer System. Bull. Am. Phys. Soc. 1956, 1, 123.

75. Schwarzl, F. R. Numerical calculation of storage and loss modulus from stress relaxation data for linear viscoelastic materials. Rheologica Acta 1971, 10, 166–173.

76. Ghosh, A.; Colby, R.H. Rouse model of star polymers. spring National ASC meeting 2008, PMSE preprints, New Orleans.

77. Liu, L.; Padding, J.; den Otter, W. K.; Briels, W. J. Coarse grained simulations of moderately entangled star polyethylene melts. J. Chem. Phys. 2013, 138, 244912.

78. Metri, V.; Louhichi, A.; Yan, J.; Matyjaszewski, K.; Baeza, G.B.; Vlassopoulos, D.; Briels, W.J. Physical networks from multifunctional telechelic star polymers: a rheological study by experiments and simulations. Macromolecules 2018, 51, 2872-2886.

79. van Ruymbeke, E.; Vlassopoulos, D.; Kapnistos, M.; Liu, CY.; Bailly, C. Proposal to Solve the Time− Stress Discrepancy of Tube Models. Macromolecules 2009, 43(1), 525-531.

80. Santangelo P. G.; Roland, M. C. Interrupted shear flow of unentangled polystyrene melts. Journal of Rheology 2001, 45, 583-594.

81. Chen, Q.; Tudryn, G.J.; Colby R. H. Ionomer dynamics and the sticky Rouse model. Journal of Rheology 2013, 57, 1441-1462.

82. Bačová P; Hawke L.G.D.; Read D.J.; Moreno A.J. Dynamics of branched polymers: A combined study by molecular dynamics simulations and tube theory. Macromolecules 2013, 46(11), 4633-4650.

For Table of Content Use only

Constraint Release mechanisms for H-Polymers Moving in Linear Matrices of varying molar masses

Helen Lentzakis, Salvatore Costanzo, Dimitris Vlassopoulos, Ralph H. Colby, Daniel Jon Read, Hyojoon Lee, Taihyun Chang, Evelyne van Ruymbeke

8.3 cm x 3.5 cm:

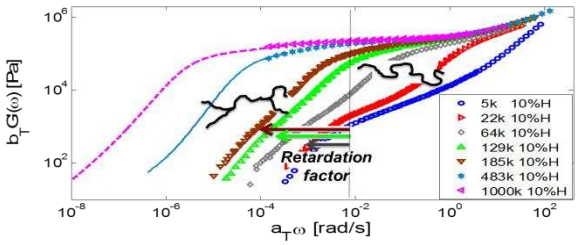

Larger picture, but same ratio: